

**LOCKHEED
CALIFORNIA
COMPANY**

THIN FILM MAGNETIC SENSOR

BURBANK, CALIFORNIA, U.S.A.



AD733702

**NATIONAL TECHNICAL
INFORMATION SERVICE**

**DDC
REFILED
DEC 13 1971
REGULATED
B**

65

UNCLASSIFIED

Security Classification

DOCUMENT CONTROL DATA - R & D

(Security classification of title, body of abstract and indexing annotation must be entered when the overall report is classified)

1. ORIGINATING ACTIVITY (Corporate author) Lockheed-California Company Burbank, California		2a. REPORT SECURITY CLASSIFICATION Unclassified	
		2b. GROUP ----	
3. REPORT TITLE Thin Film Magnetic Sensor - Final Report			
4. DESCRIPTIVE NOTES (Type of report and inclusive dates) Final Report - Phase I			
5. AUTHOR(S) (First name, middle initial, last name) Frank J. Fuller			
6. REPORT DATE 30 September 1971		7a. TOTAL NO OF PAGES 65	7b. NO OF REFS 2
8a. CONTRACT OR GRANT NO N00014-71-C-0298		9a. ORIGINATOR'S REPORT NUMBER(S) LR 24792	
b. PROJECT NO. NR 220-038/02-17-71		9b. OTHER REPORT NO(S) (Any other numbers that may be assigned this report)	
c.			
d.			
10. DISTRIBUTION STATEMENT Approved for Public Release; Distribution Unlimited.			
11. SUPPLEMENTARY NOTES		12. SPONSORING MILITARY ACTIVITY Office of Naval Research (Code 461) Department of the Navy Arlington, Virginia 22227	
13. ABSTRACT <p>This final report covers the work conducted under this first phase of the above contract for ONR. The objectives were two-fold: (1) Comparison tests of a thin film sensor and the present production aircraft magnetic anomaly detector (MAD) the AN/ASQ-81. (2) Preliminary tests of the basic concept of three axis sum/square motion compensation.</p> <p>The results of this program indicated first task feasibility toward a small, low power, motion compensated sensor. A rod sensor was utilized in lieu of a thin flat chip element because it provided free magnetic pole characteristics, a simplified method for 3-axis symmetry, more probable mechanical reliability, and mutually independent sensor operation.</p> <p>Comparison testing indicated a thin film sensor performance, as expected, below ASQ-81 performance of the order of one quarter the range. However, data presented indicates a range ratio probability of one-half or better. The results of the 3-axis motion compensation tests using arithmetical computation of the sum/square function produced a motion compensated output.</p>			

UNCLASSIFIED

Security Classification

14

KEY WORDS	LINK A		LINK B		LINK C	
	ROLE	WT	ROLE	WT	ROLE	WT
Thin Film Magnetic Sensor Magnetic Sensor Thin Film Sensor vs ASQ-81 Comparison MAD Detectors Motion Compensation 3-Axis Motion Compensation						

DD FORM 1473 (BACK)
1 NOV 68
(PAGE 2)

UNCLASSIFIED
Security Classification

LOCKHEED CALIFORNIA COMPANY

REPORT NO. LR 24792
DATE 30 SEPTEMBER 1971
MODEL _____
COPY NO. 000027

TITLE FINAL REPORT
THIN FILM MAGNETIC SENSOR

REFERENCE ONR CONTRACT AUTHORITY NR 220-038/02-17-71
CONTRACT NUMBER (S) N00014-71-C-0298

THIS RESEARCH WAS
SPONSORED BY:

OFFICE OF NAVAL RESEARCH
AERONAUTICS, CODE 461
ARLINGTON, VA. 22217

PREPARED BY *F. J. Fuller*
F. J. Fuller
Principal Investigator

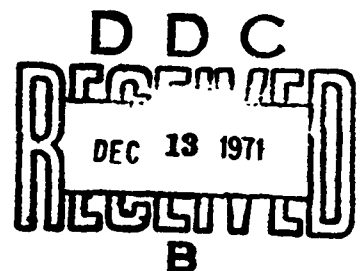
APPROVED BY *T. G. Shaw*
T. G. Shaw - Group Engineer
Development, Avionics Laboratory

APPROVED BY *D. E. Walters*
D. E. Walters
ASW R and D Systems Engineer

APPROVED BY *D. A. Unger*
D. A. Unger - Dept. Engineer
Avionics Laboratory

APPROVED BY *D. R. Meyer*
D. R. Meyer - Division Engineer
Avionic Systems Division

APPROVED FOR PUBLIC RELEASE; DISTRIBUTION UNLIMITED.



THIN FILM MAGNETIC SENSOR
FOREWORD/ABSTRACT

This report describes the work conducted under the Thin Film Magnetic Sensor research program executed for the Office of Naval Research under Contract N00014-71-C-0298. This contract calls for comparison tests using a single axis thin film sensor and the AN/ASQ-81 Magnetic Anomaly Detector plus preliminary tests of the basic three axis sum/square motion compensation concept. The results of this program indicate first task feasibility toward a small, low power, motion compensated sensor.

The sum/square motion compensation concept was based upon a common phase reference for excitation of three mutually perpendicular sensors; this concept dictated the use of an externally pumped thin film sensor for the sensitivity comparison testing under this contract.

A rod sensor was utilized in lieu of a thin flat square chip element because it provides free magnetic pole characteristics, a simplified method for 3-axis symmetry, more probable mechanical reliability, and mutually independent sensor operation; all of these characteristics are required for either compass or MAD applications of a final 3-axis motion compensated sensor configuration.

Comparison testing indicated that at this early stage of externally pumped rod development, sensor performance is as expected below ASQ-81 performance; i.e., a nominal thin film to ASQ-81 range

ratio of 1/4. However, data presented herein indicates in terms of achieved square chip performance a range ratio probability on the order of 1/2 or better. The high and variable characteristics of environmental noise in the Burbank area (air traffic, surface traffic, plant and industrial noise sources) precluded accurate comparisons of system performance. Numerous shutdowns occurred because of AN/ASQ-81 production installation tests. No thin film failures occurred; however, thin film performance varied because of the environmental noise and the critical operation of the unshielded high impedance pump presently used. For these reasons, the comparison testing in Burbank was made on the basis of signal to noise ratio comparisons while minimum discernible (MDS) range comparisons were made at the Rye Canyon Research facility because of its more secluded and relatively quiet environment.

The fundamental concept (3-axis sum/square motion compensation) was tested using the AN/ASA-65 rod system since it was available, is a standard unit in production, would meet the basic common pump phase reference requirement, and because it would simulate the feasibility of the concept. The results of these tests indicated concept validity. Mutually independent sensor operation provided the necessary phase trigonometric relations among the three sensor rod outputs. As a result, arithmetical computation of the sum/square function produced a motion compensated output while the individual sensor outputs showed typical sine function response as a function of orientation angle.

The intent of the contract for basic comparison and motion compensation objectives were met during the program. Further,

since reliability problems were a source of concern in ASQ-81 production programs, some of the originally planned comparison testing time was applied towards more detailed test data on electronic squaring circuitry, pump noise sources, rod sensor refinements and pump noise reduction.



TABLE OF CONTENTS

	Page No.
FOREWORD/ABSTRACT	ii
TABLE OF FIGURES	vi
INTRODUCTION	1
TEST FACILITIES	2
SENSITIVITY COMPARISON TEST DATA	4
ROD SENSOR POTENTIAL	28
MOTION COMPENSATION 3-AXIS SUM/SQUARE DATA	30
General	30
Vertical Axis Data	30
3-Axis Skew Data	35
Squaring Circuit Development	37
DISCUSSION: RESULTS, PROBLEM AREAS AND SOLUTIONS	39
CONCLUSIONS	46
RECOMMENDATIONS	47
BIBLIOGRAPHY	49
APPENDIX A: FACILITY/TEST PHOTOGRAPHS	A-1

TABLE OF FIGURES

Figure No.		Page No.
1	Low Height Field Fixture (Rye Canyon Test Facility)	3
2	Gamma Slinger Comparison Data - 5 ft. & 10 ft. (Burbank Tests)	7
3	Gamma Slinger Comparison Data - 20 ft. & 40 ft. (Burbank Tests)	8
4	Environmental Noise - Morning	9
5	Environmental Noise - Afternoon & Evening	10
6	Environmental Noise - Morning, Near Ground	11
7	Environmental Noise - Afternoon, Evening, Near Ground	12
8	Environmental Noise - Evening, Above Ground	13
9	Gamma Slinger Comparison Data - Near Ground (Burbank Tests)	14
10	Track Test Comparison Data	15
11	Rye Canyon Near Ground Test Data ASQ-81 & Thin Film in Close Proximity Gamma Slinger - 3 ft to 4 ft.	16
12	Rye Canyon Near Ground Test Data ASQ-81 & Thin Film in Close Proximity Gamma Slinger @ 4 ft. 6 in.	17
13	Rye Canyon Near Ground Test Data ASQ-81 & Thin Film in Close Proximity Gamma Slinger @ 5 ft.	18
14	Rye Canyon Near Ground Test Data ASQ-81 & Thin Film Separated Gamma Slinger @ 16 ft & 30 ft.	19
15	Rye Canyon - Near Ground Test Data Gamma Slinger @ 18 ft. & 21 ft.	20
16	Rye Canyon Near Ground Test Data Gamma Slinger @ 24 & 27 ft.	21
17	Rye Canyon Near Ground Test Data Gamma Slinger @ 16 ft. 40 ft. and 50 ft.	22
18	Rye Canyon Balloon Test Data Gamma Slinger 5 ft. and less	23
19	Rye Canyon Balloon Test Data Gamma Slinger 45 ft. - 50 ft.	24

TABLE OF FIGURES (Cont)

Figure No.		Page No.
20	Thin Film/Target Orientation Data N, NE, E & SE Target North of Thin Film	25
21	Thin Film/Target Orientation Data S, SW, W & NW Target South of Thin Film	26
22	Self-Pumped Square Chip Data Samples (No Motion Compensation)	29
23	3-Axis Test Data (One Axis Vertical)	31
24	Graph of 3-Axis Skew Sum/Square Data	32
25	3-Axis Concept Validation Data (V-Axis: Vertical)	33
26	3-Axis Concept Validation Data (V-Axis Skewed)	34
27	3-Axis Derivative Coupling Data	36
28	Typical Squaring Circuit Data	38
29	Self-Pumped Thin Film Data	40
30	Pump/Sensor Feedback	41
31	Bipolar Output Characteristics	43
A-1	Exterior - Rye Canyon Balloon Magnetics Test Facility	A-2
A-2	Magnetics Test and Control Building (Rye Canyon Test Facility)	A-3
A-3	Balloon Interior Maneuver Cradle with ASQ-81 & Thin Film Sensor	A-4
A-4	Model Target Track (Burbank Test Facility)	A-5
A-5	Model Target Track Closeup (Burbank Test Facility)	A-6

BLANK PAGE

INTRODUCTION

This report describes the work conducted under the ONR "Thin Film Magnetic Sensor" contract N00014-71-C-0298. The fundamental objectives of the contract were attained. The objectives being: (1) comparison tests in different noise environments between the AN/ASQ-81 P-3C and S-3A MAD (Magnetic Anomaly Detector) and the thin film sensor and (2) initial three axis sum/square motion compensation feasibility tests.

Comparison tests were conducted on the field of the Hollywood-Burbank airport and also at the Lockheed Rye Canyon Research Facility Magnetics Laboratory area. Both series of tests were run at different periods of the day and night and at various heights off the ground to permit a wide variance in the noise environment.

The following pages of this report depict the test facilities and setups used in this program, sensitivity comparison data, 3-axis sum/square data, results of other tests conducted, conclusions and recommendations.

TEST FACILITIES

The Rye Canyon field test setup used in this program is shown in Figure 1 with an insert of a closeup of the test units in the upper right hand corner. The cylindrical configuration is the AN/ASQ-81 and the three axis thin film rod sensor is shown next to the ASQ-81 sensor head. All structures and fixtures used were of non-magnetic materials. Figure 1 also shows the ASQ-81 compensation coil setup on the ground below the sensors and a gamma slinger (rotating magnetic with a rated moment of 1045 c.g.s. units) in the foreground. Appendix A includes related test setup photographs illustrating the various Burbank and Rye Canyon facilities used in this program.

SENSITIVITY COMPARISON TEST DATA

The sensitivity comparison data taken were reasonably consistent although there were considerable variance in the data. Figures 2 and 3 illustrate Burbank gamma slinger data in which the ASQ-81 shows at a distance of 20 feet a signal to noise ratio approximately equal to that of the thin film at 5 feet. This implies a thin film to ASQ-81 range ratio of a little better than 1/4. For the thin film, the peak-to-peak response at 5 feet was quite discernible whereas 10 feet shows a non-discernible response; therefore, it is apparent from these tests that the thin film rod minimum discernible range lies between 5 and 10 feet. On the other hand, the ASQ-81 showed significant differences between responses at 3 P.M. and at 4 P.M.. The 20 foot ASQ-81 data indicates a signal to noise ratio which on the basis of cube law physics would not extrapolate much beyond the 20 foot reliable range. While an ASQ-81 temperature failure prevented continuation of this particular test, it was obvious that the relative range ratio is better than 1 to 4.

Because of the difficulty of analytically relating these data to cube law principles, a series of tests were run to check how the outputs of both systems varied with respect to environmental noise. Figures 4 through 8 show ASQ-81 response to environmental noise variations while the thin film shows no such response. These results indicated the difficulty of true relative system sensitivity comparisons in the high level Burbank noise environment. Further, comparisons tended to distort the true capability of the ASQ-81 and indicated the need for quiet environment testing. However, some additional gamma slinger

tests were run in the Burbank area when such tests did not interfere with ASQ-81 production testing. Figure 9 is an example which shows considerably better thin film signal to noise ratio at 5 feet than illustrated in Figure 2; this particular test was curtailed however, because of ASQ-81 failure and subsequent production testing.

Figure 10 illustrates typical submarine model track test data taken from runs conducted on the Target Model Track Test Facility. The thin film was approximately at minimum discernible signal (MDS) while the ASQ-81 provided a signal to noise ratio of 40/2 or 20 to 1. Thus, the relative signal to noise ratio superiority of the ASQ-81 was, for these tests, 20 to 1 which in accordance with the cube law provides a relative thin film to ASQ-81 range ratio of about 1 to 2.7. Attempts to conduct further tests on the track at different model ranges at this time were aborted because of ASQ-81 production aircraft problems. Because of the difficulty in securing additional data caused by Burbank production testing for delivery aircraft and the need for a quiet environment, the testing was transferred to Rye Canyon.

Rye Canyon test procedures were compromised by continuing ASQ-81 reliability requirements for production testing. However, tests were conducted when schedules permitted. No thin film failures occurred so this was not a factor.

Figures 11, 12, and 13 show a low but significant variance in thin film performance with the gamma slinger turned on and off at distances up to 5 feet. The ASQ-81 was turned on but showed no response; a series of tests showed that because of interference

the thin film sensor had to be placed at least 2 feet from the ASQ-81 sensor head in order to secure proper ASQ-81 operation and this 2 feet was used on all subsequent tests.

In Figure 14 the ASQ-81 shows very erratic performance at 30 feet, but discernible performance at 16 feet and the thin film not at all. Figure 15 shows erratic but discernible ASQ-81 performance at 18 and 21 feet. Figures 16 and 17 show a minimum discernible ASQ-81 range of 24 feet. On the basis of Figure 13 thin film MDS at 6 feet this indicates a relative range ratio of $6/24 = 1/4$. However, it is apparent that even in the less noisy Rye Canyon environment the data is still statistically noisy.

The data taken with the gamma slinger and the thin film sensor mounted on the maneuver boom above ground inside the balloon, and shown in Figure 18, shows a small difference in thin film response with the gamma slinger turned on and off at a distance of 5 feet; 6 feet would probably be close to MDS. Figure 19 shows a performance variation for the ASQ-81 at 45 feet that is at one time discernible and at another time not discernible. At greater distances up to 50 feet, no discernible signal occurred as there were noise pulses which exceeded any possible signal by 10 db. At this point, the ASQ-81 failed. As a result, the tests were terminated because of adverse reliability effects on production testing. These data indicate a range ratio of $6/45 = 1$ to 7.5.

The effect of the gamma slinger target orientation with respect to the thin film sensor in compass heading reference is shown in Figures 20 and 21. From these data the conclusion can be drawn

GAMMA SLINGER COMPARISON DATA - 5 ft. & 10 ft.
(BURBANK TESTS)

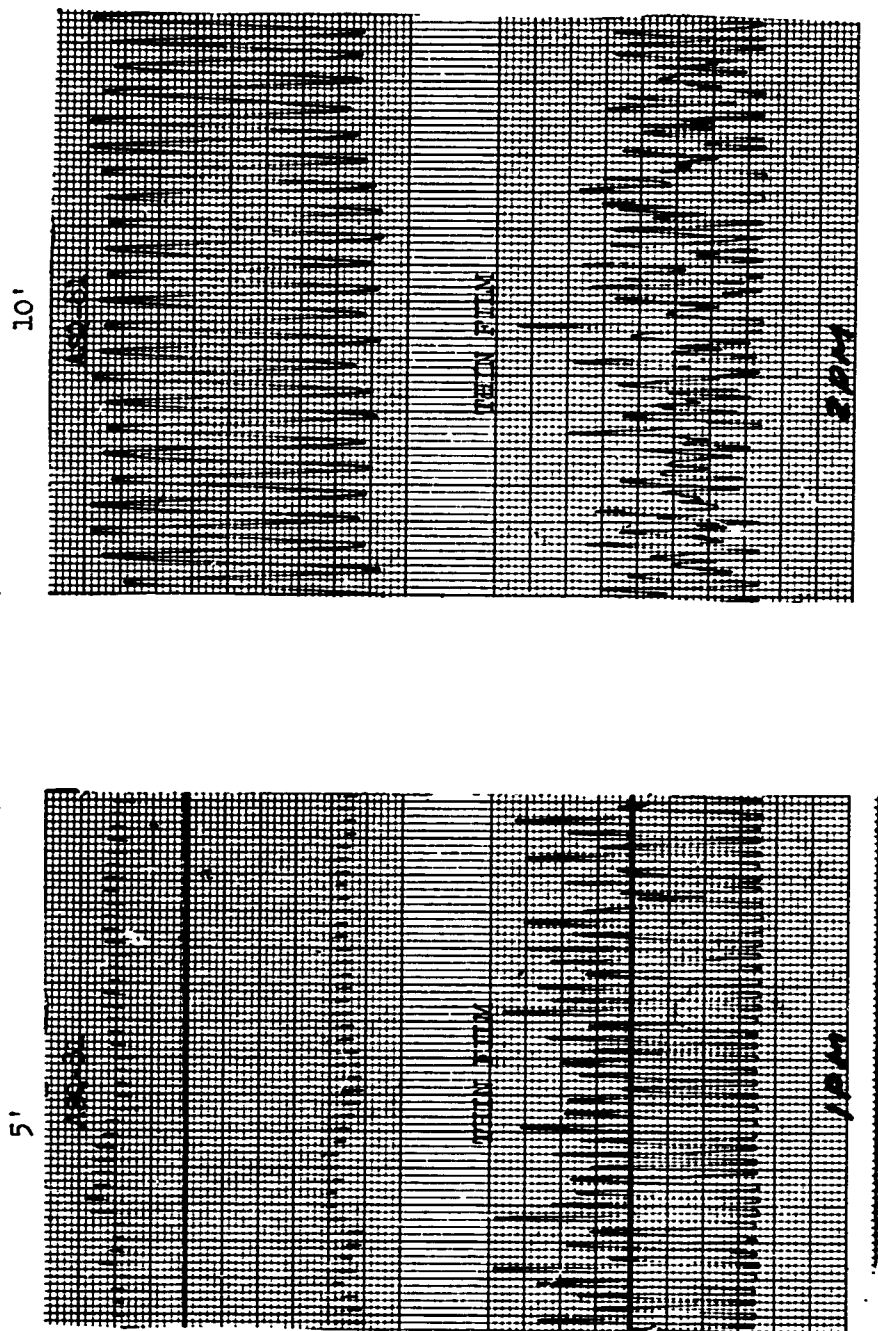
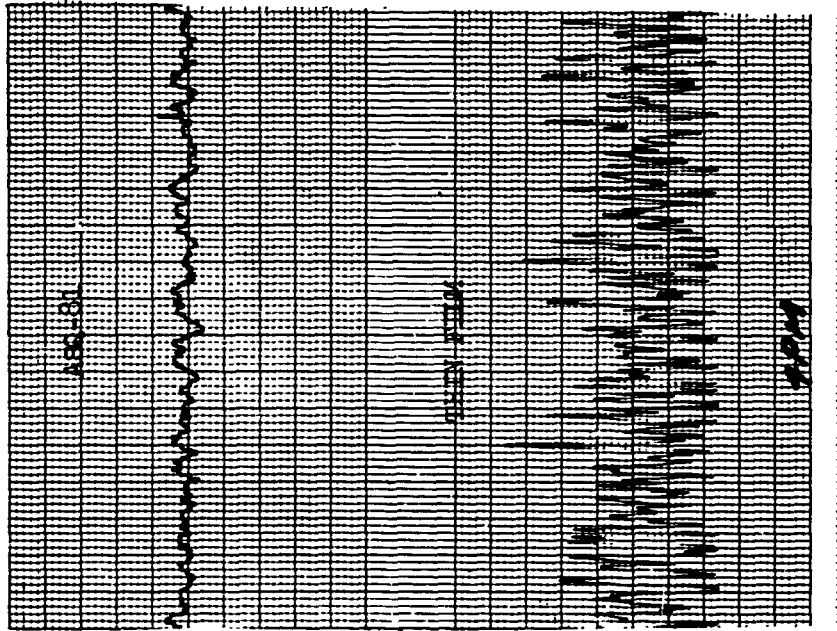


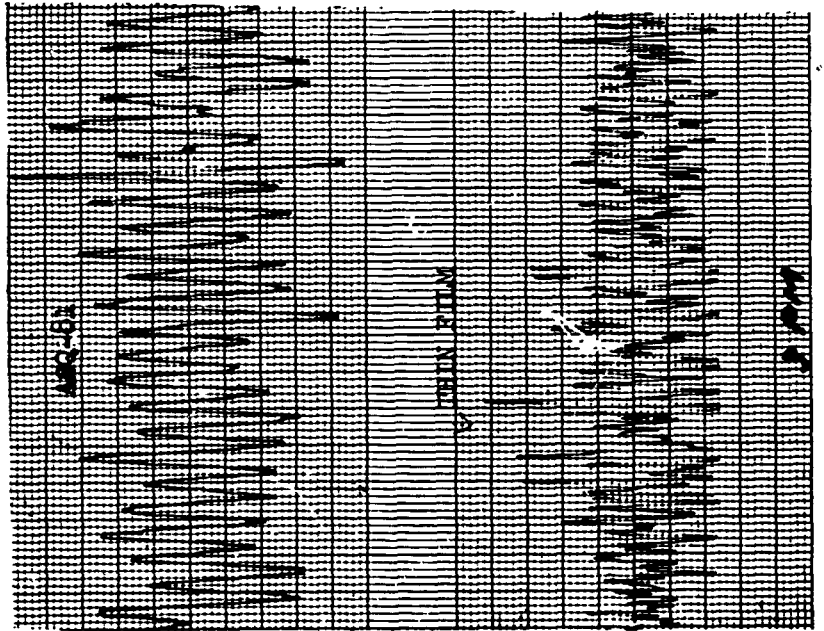
FIGURE 2

GAMMA SLINGER COMPARISON DATA - 20 FT. & 40 FT.
(BURBANK TESTS)

40'



20'

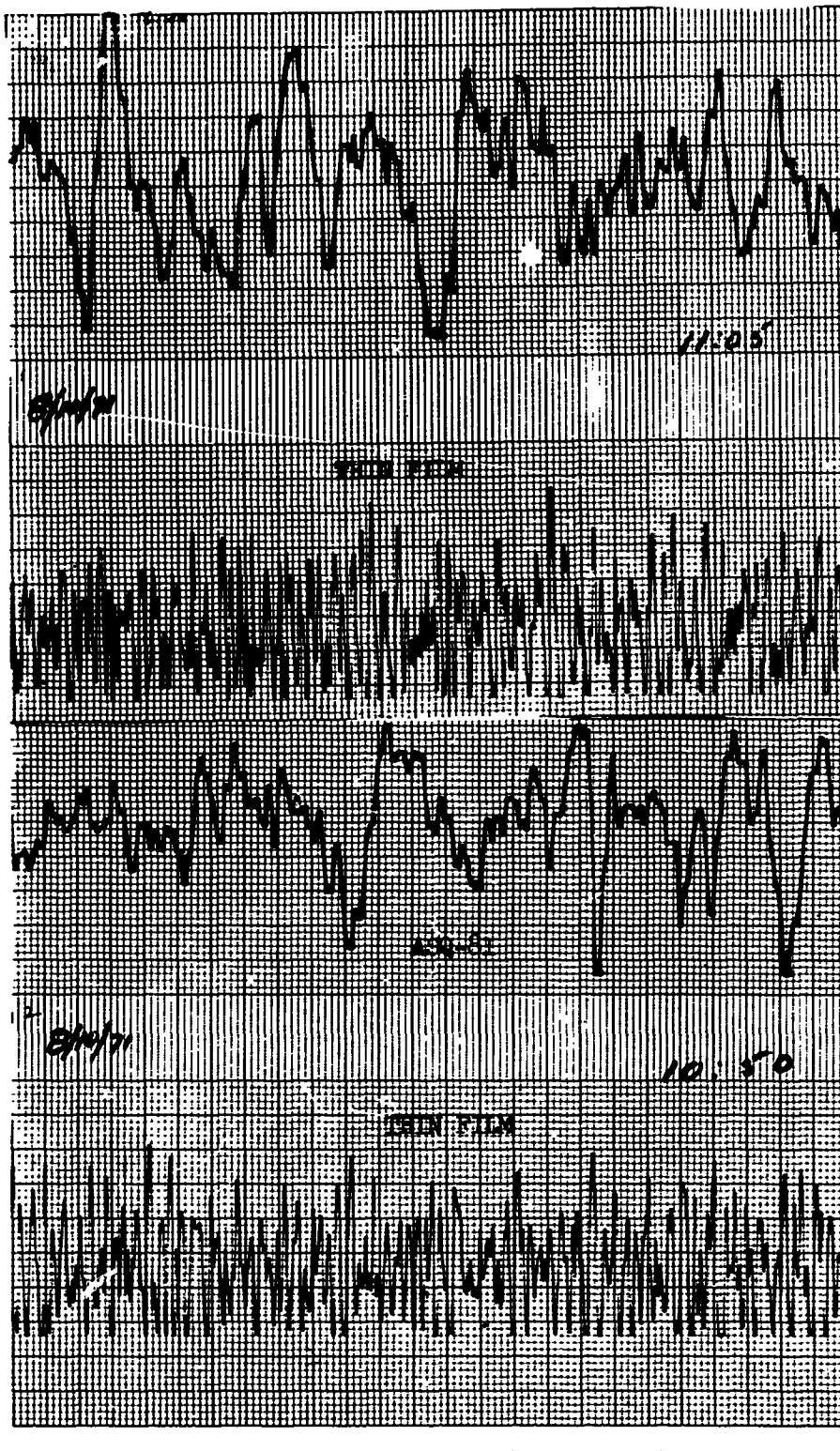


→ TIME (mm/sec.)

→ TIME (mm/sec.)

FIGURE 3

ENVIRONMENTAL NOISE - MORNING

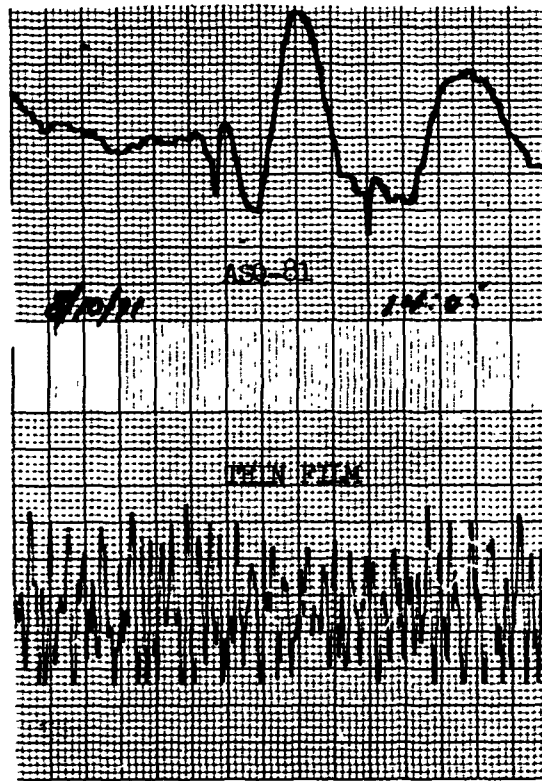
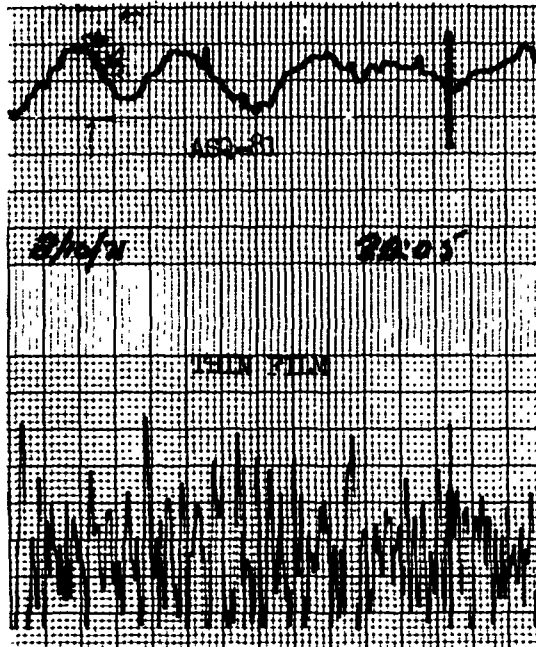


→ TIME (mm/sec.)

FIGURE 4



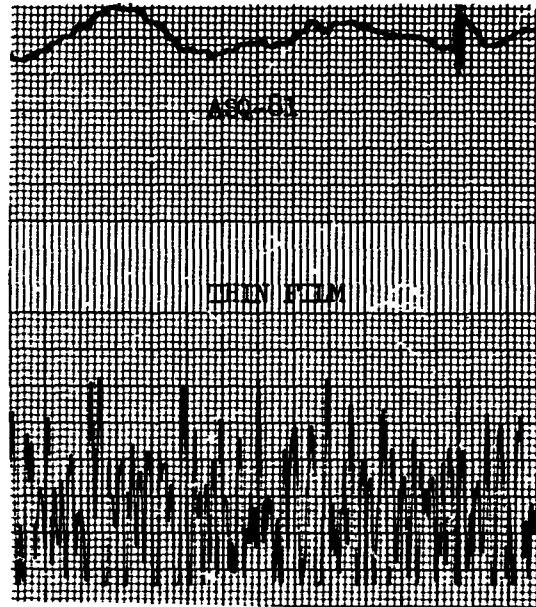
ENVIRONMENTAL NOISE - AFTERNOON & EVENING



→ TIME (min/sec.)
FIGURE 5



ENVIRONMENTAL NOISE - MORNING, NEAR GROUND

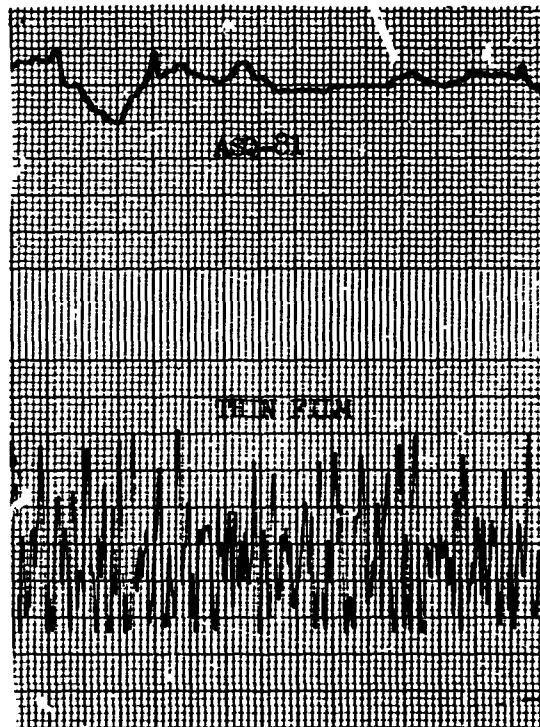


8-13-71

HEIGHT 3'6"

10:05 A.M.

→ TIME (mm/sec.)



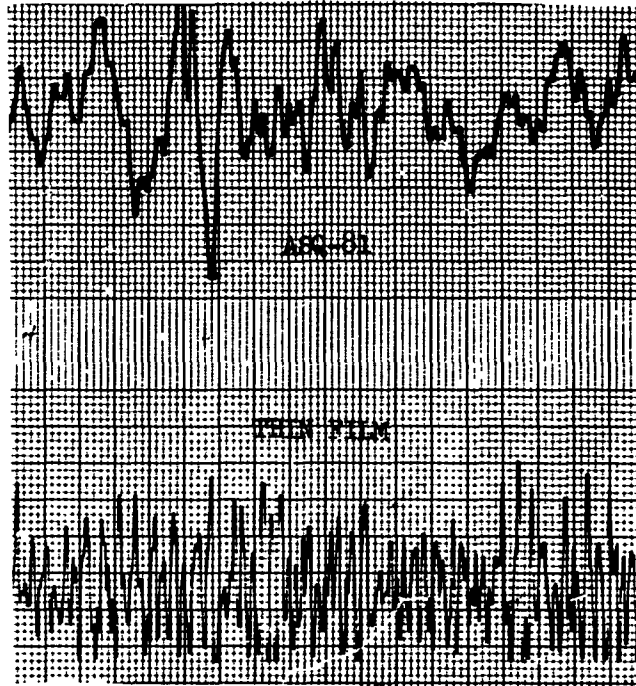
8-13-71

HEIGHT 3'6"

12:00

FIGURE 6

ENVIRONMENTAL NOISE - AFTERNOON, EVENING, NEAR GROUND



8-13-71

HEIGHT 3' 6"

16:30

→ TIME (mm/sec.)



8-13-71

HEIGHT 3' 6"

19:30

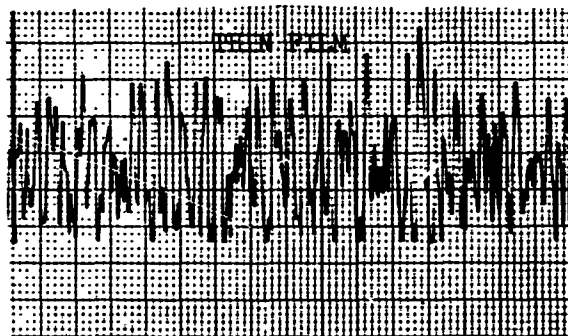
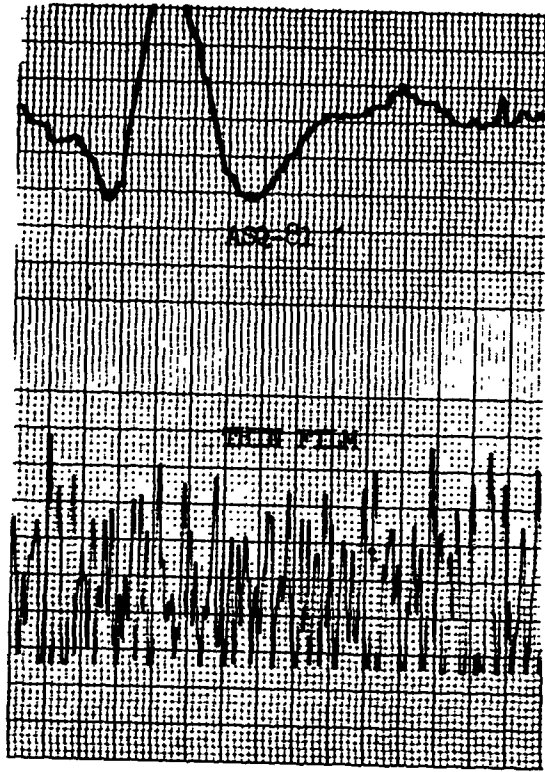


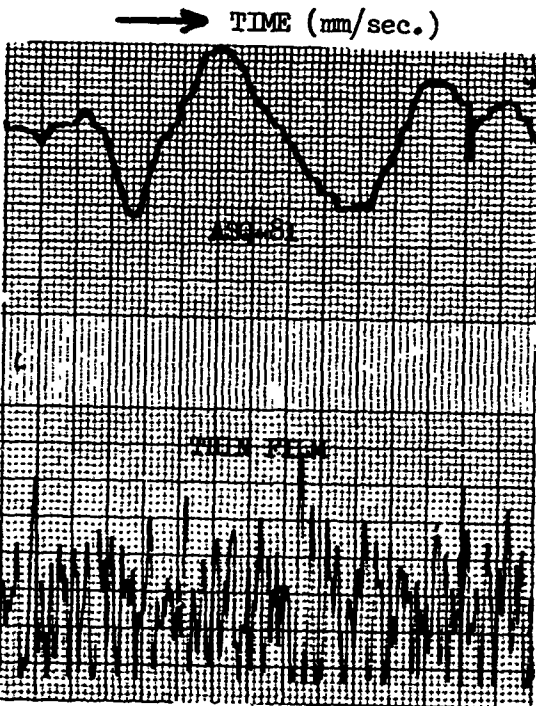
FIGURE 7

IR 24792

ENVIRONMENTAL NOISE - EVENING, ABOVE GROUND



8-13-71
HEIGHT 16'
19:45

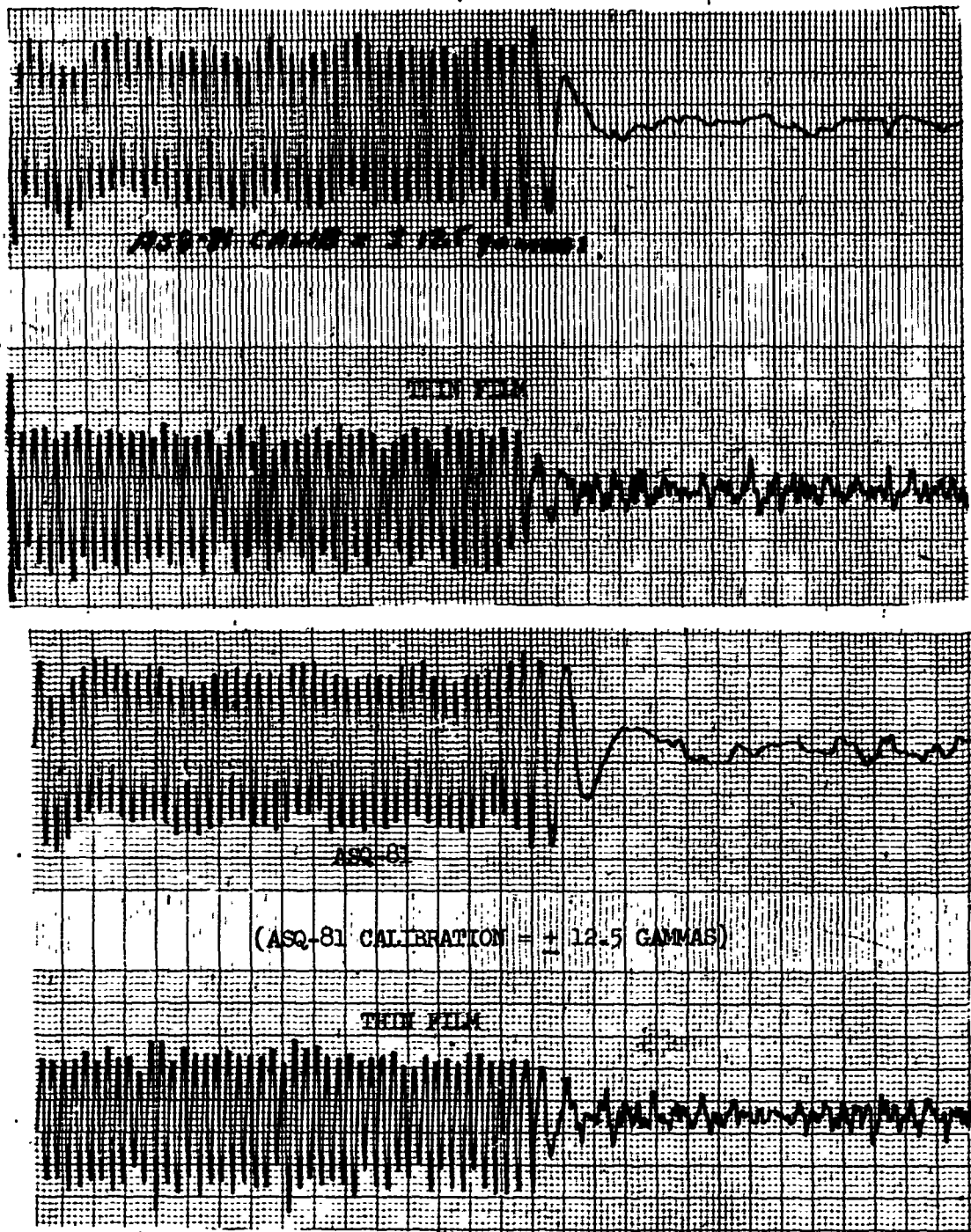


8/13/71
19:50

FIGURE 8
13

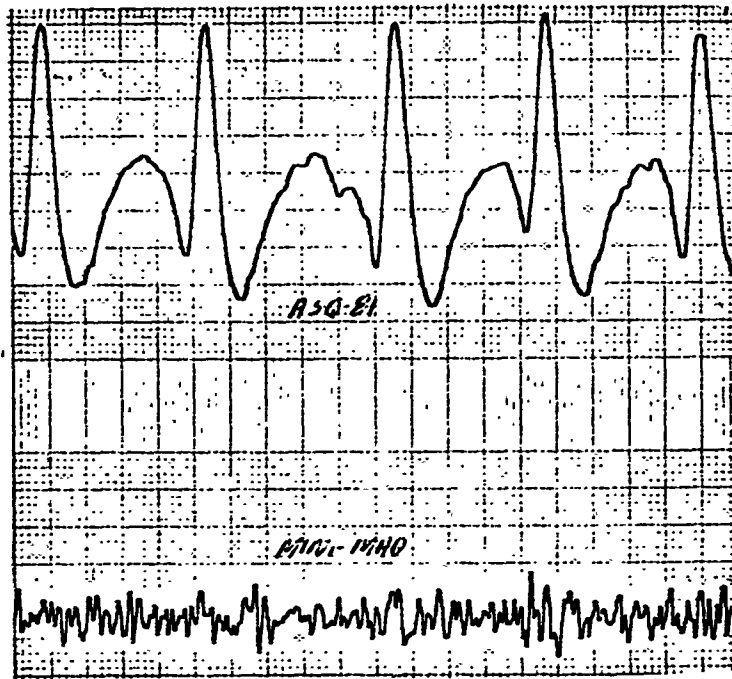


GAMMA SLINGER COMPARISON DATA - NEAR GROUND (BURBANK TESTS)



→ TIME (mm/sec.)
FIGURE 9

TRACK TEST COMPARISON DATA



→ TIME (mm/sec.) 7/2/71

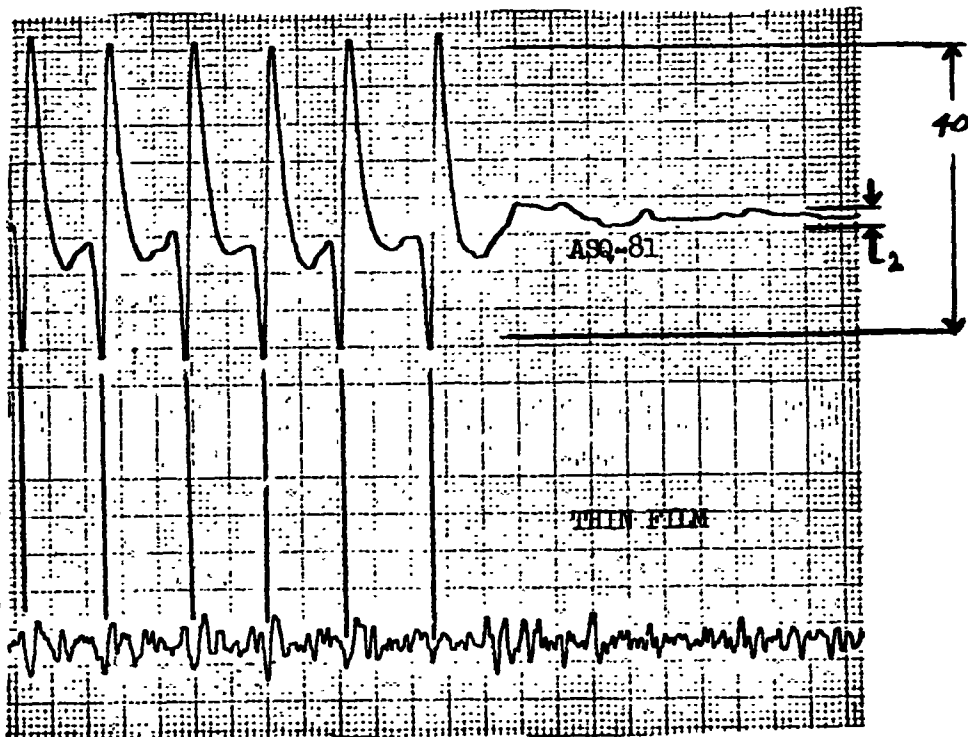
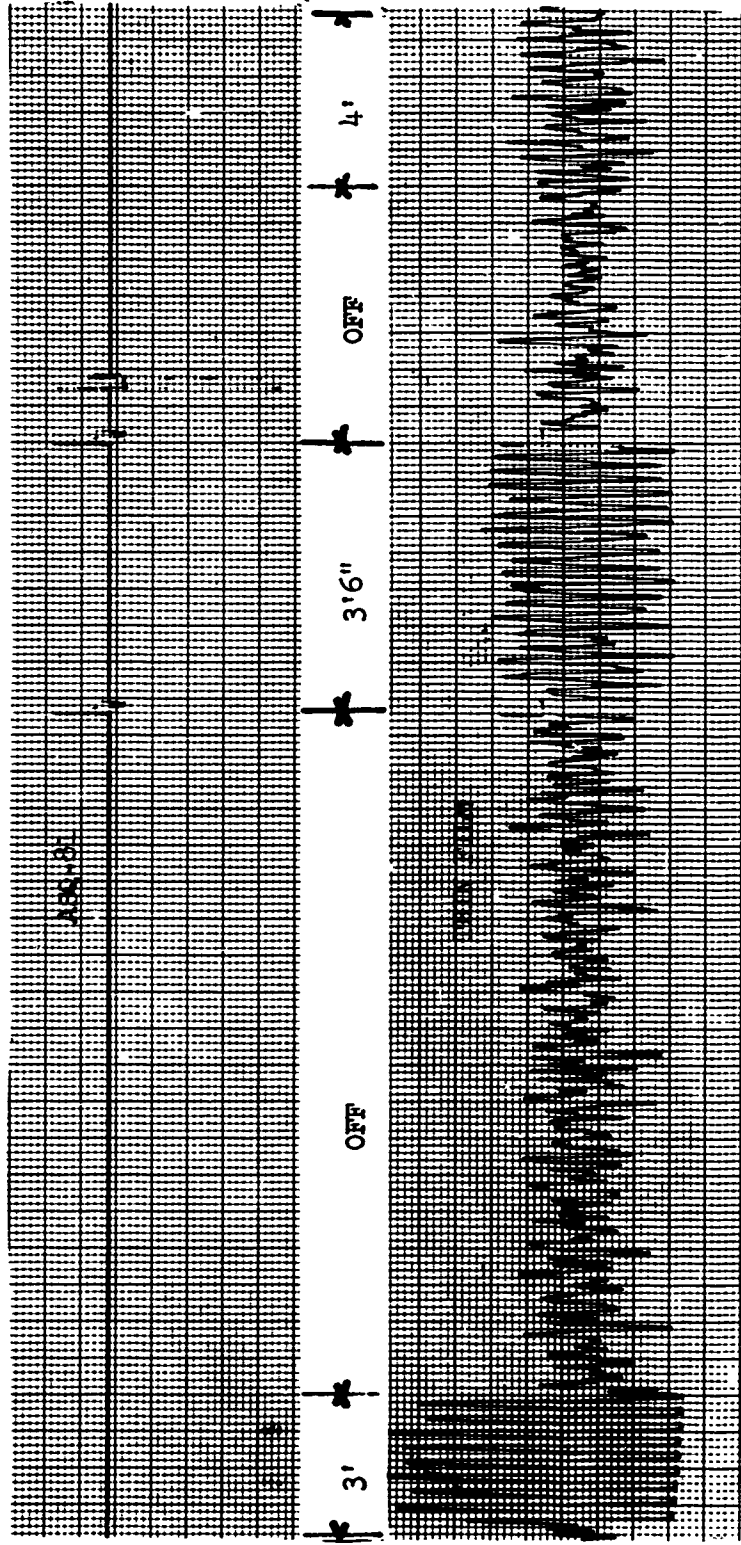


FIGURE 10



RYE CANYON NEAR GROUND TEST DATA
ASQ-81 & THIN FILM IN CLOSE PROXIMITY
GAMMA SLINGER - 3 FT TO 4 FT.



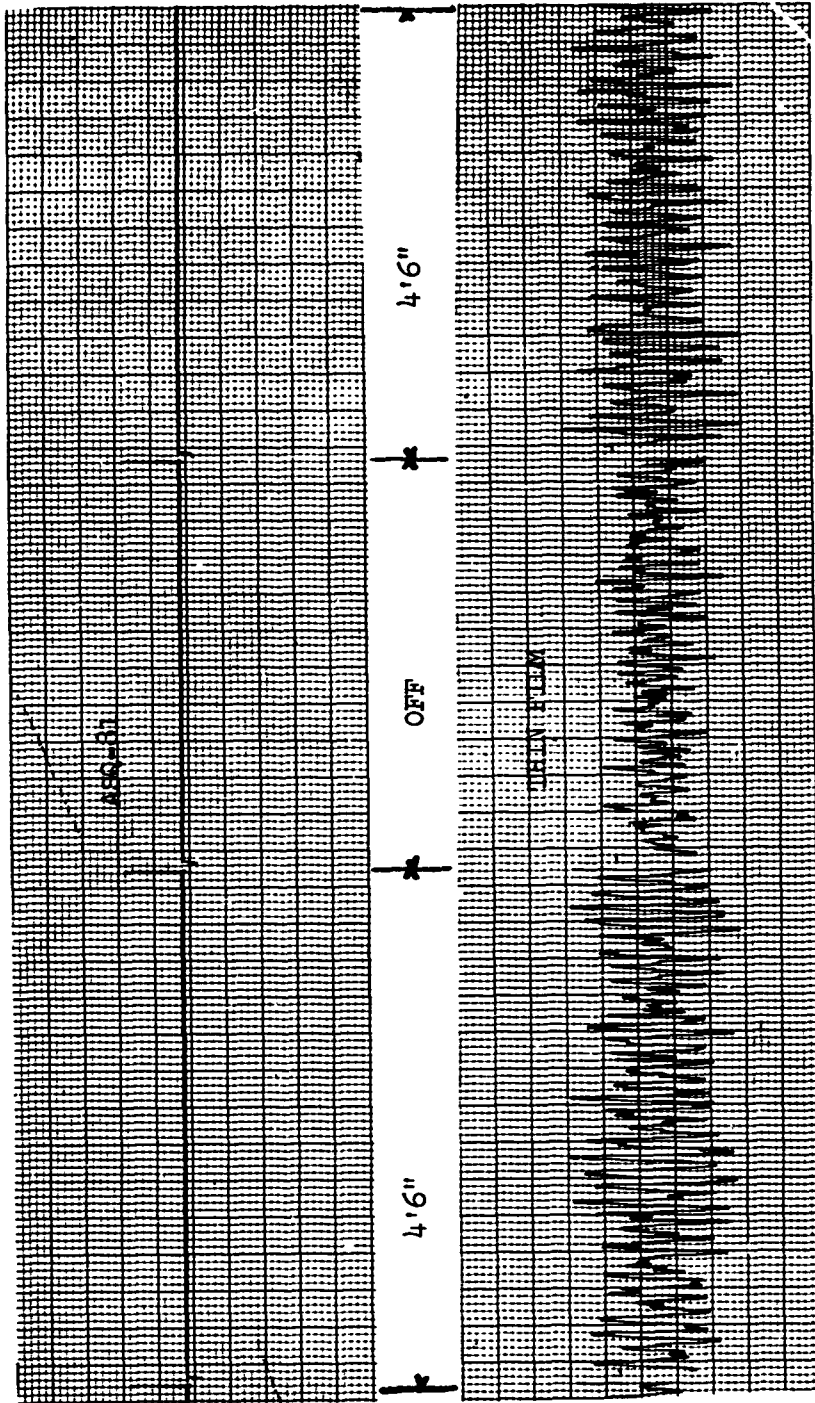
↑ TIME (mm/sec.)

6 P.M. - 8 P.M.

FIGURE 11



RYE CANYON NEAR GROUND TEST DATA
ASQ-81 & THIN FILM IN CLOSE PROXIMITY
GAMMA SLINGER @ 4 FT. 6 IN.

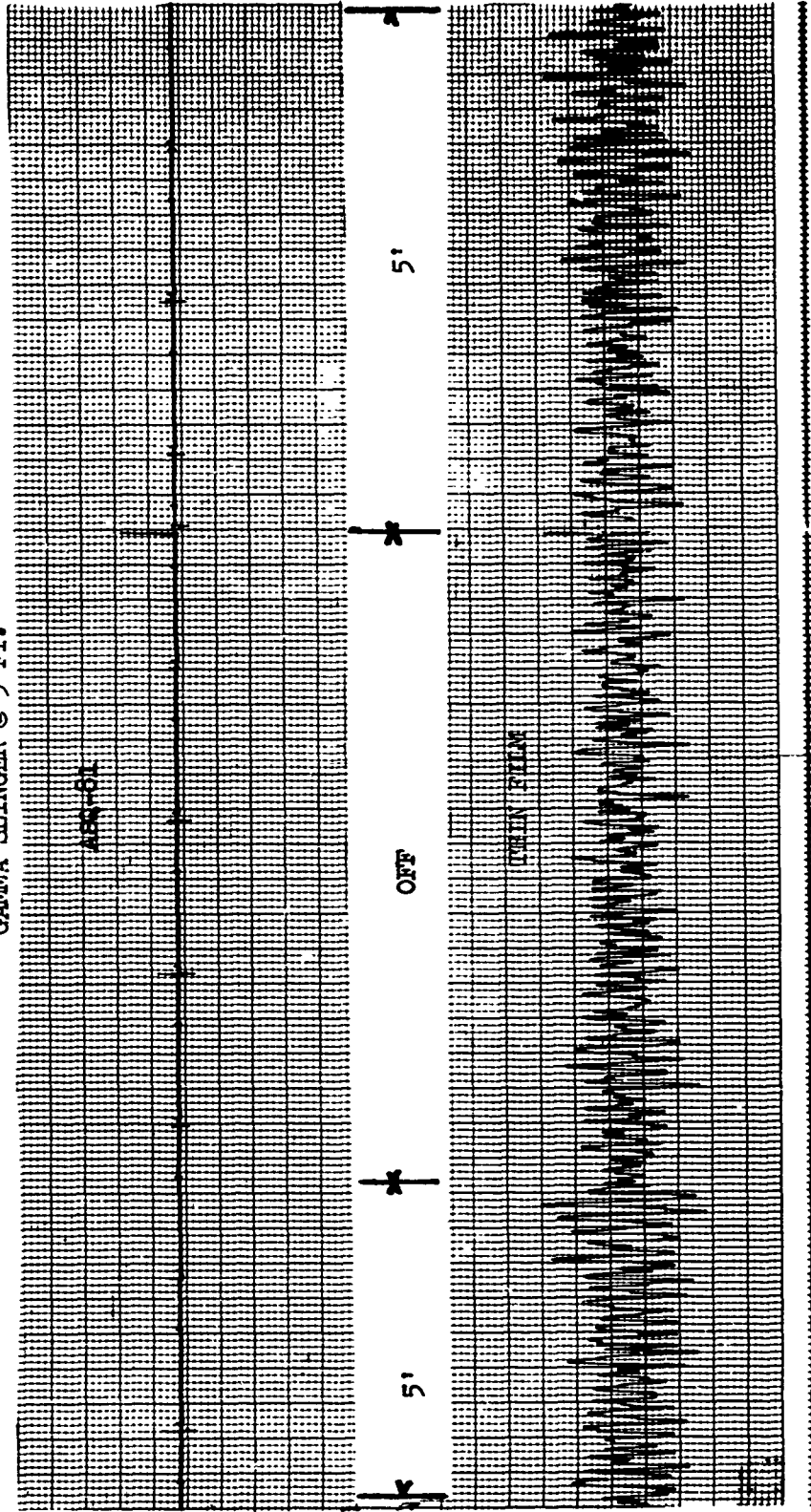


TIME (mm/sec.)

6 P.M. - 8 P.M.

FIGURE 12

EYE CANYON NEAR GROUND TEST DATA
ASQ-81 & THIN FILM IN CLOSE PROXIMITY
GAMMA SLINGER @ 5 FT.

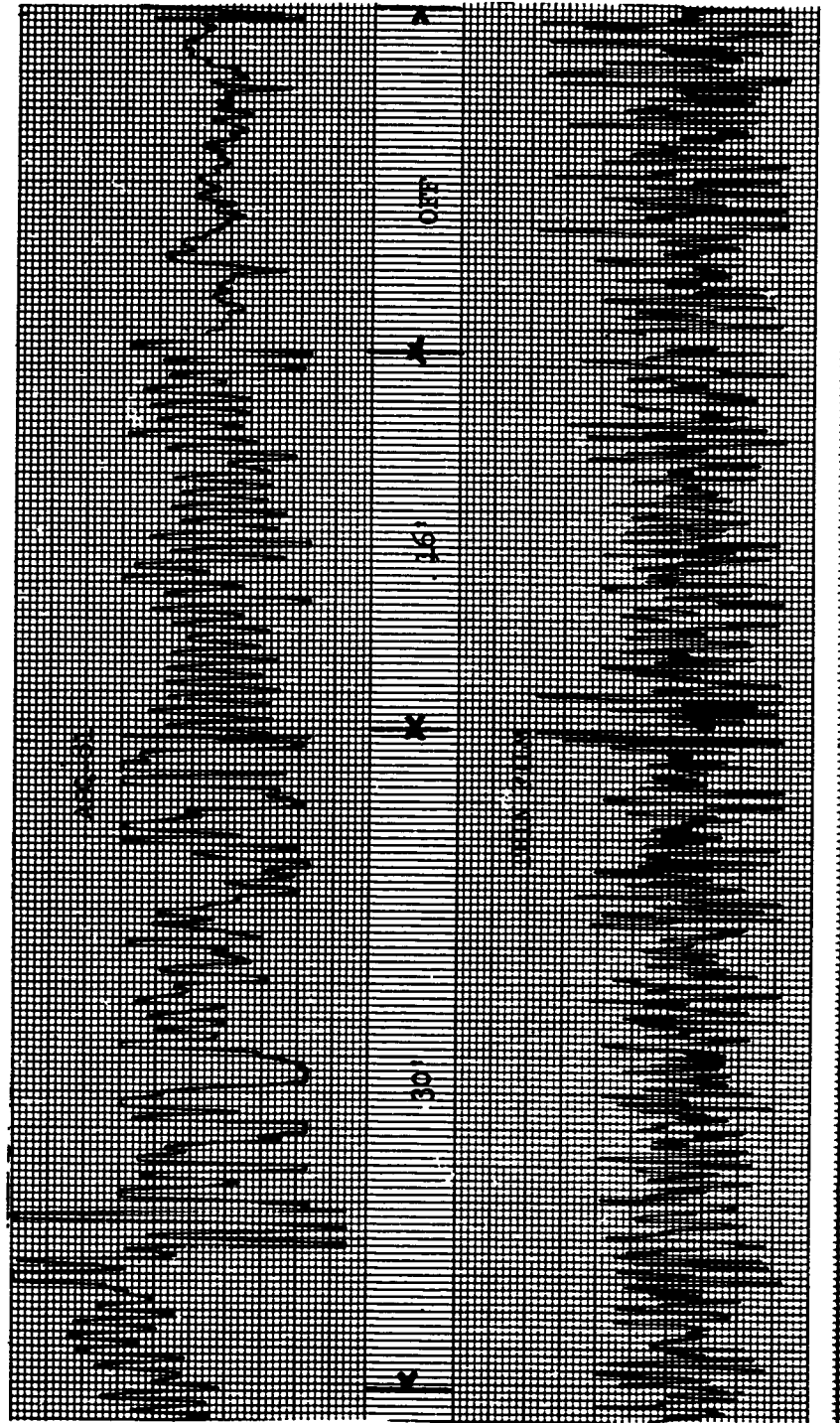


6 P.M. - 8 P.M.

FIGURE 13



RYE CANYON NEAR GROUND TEST DATA
ASQ-81 & THIN FILM SEPARATED
GAMMA SLINGER @ 16 FT & 30 FT

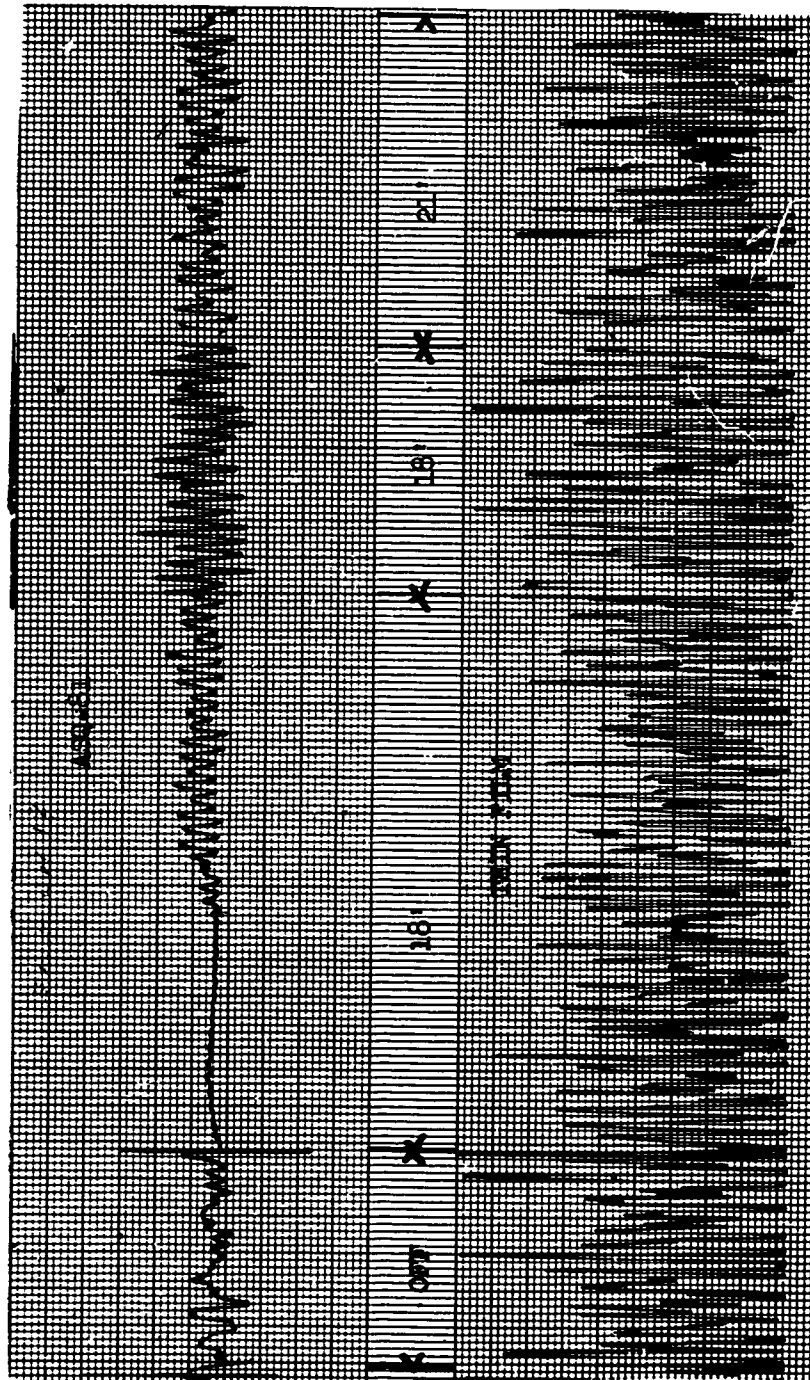


8 P.M. - 11 P.M.

FIGURE 14



RYE CANYON - NEAR GROUND TEST DATA
GAMMA SLINGER @ 18 FT & 21 FT

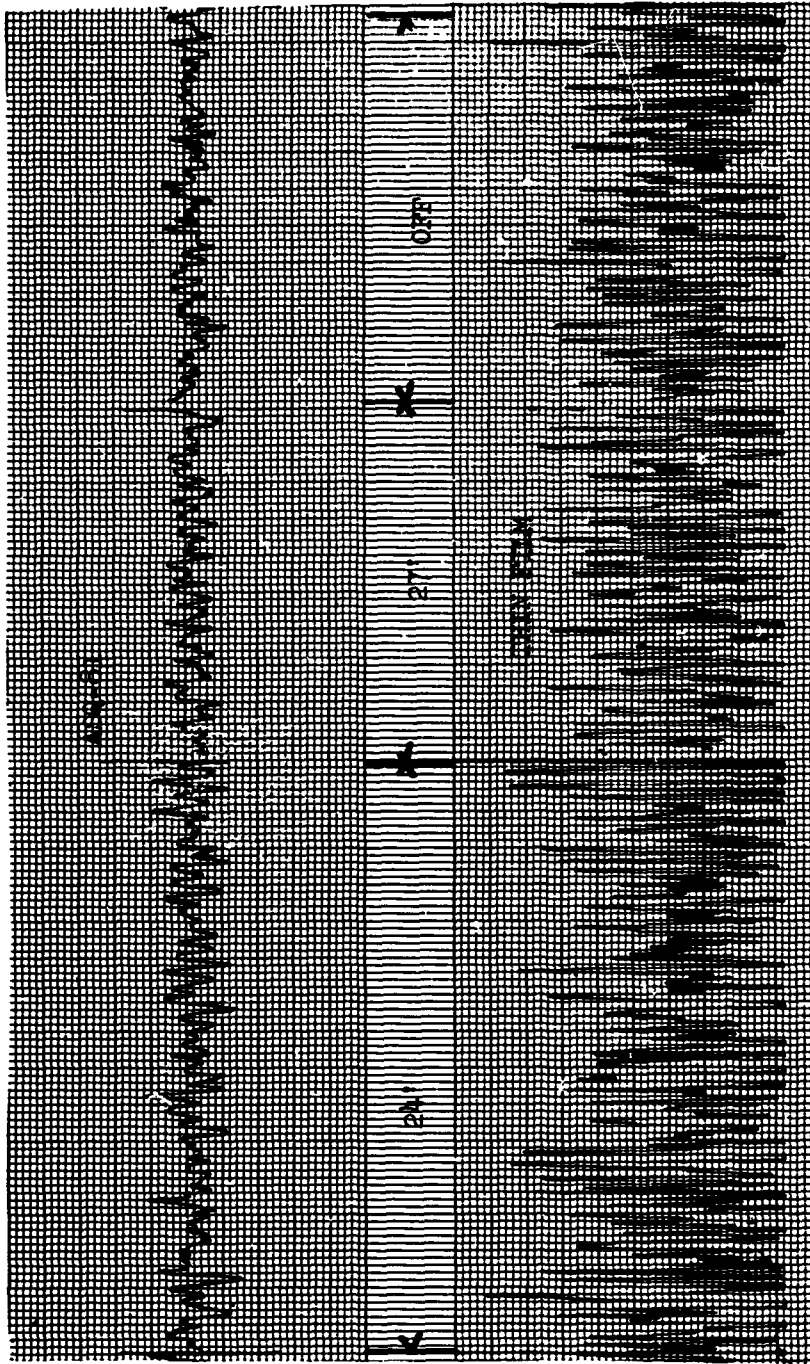


TIME (mm/sec.)

8 P.M. - 11 P.M.

FIGURE 15

RYE CANYON NEAR GROUND TEST DATA
GAMMA SLINGER @ 24 FT & 27 FT



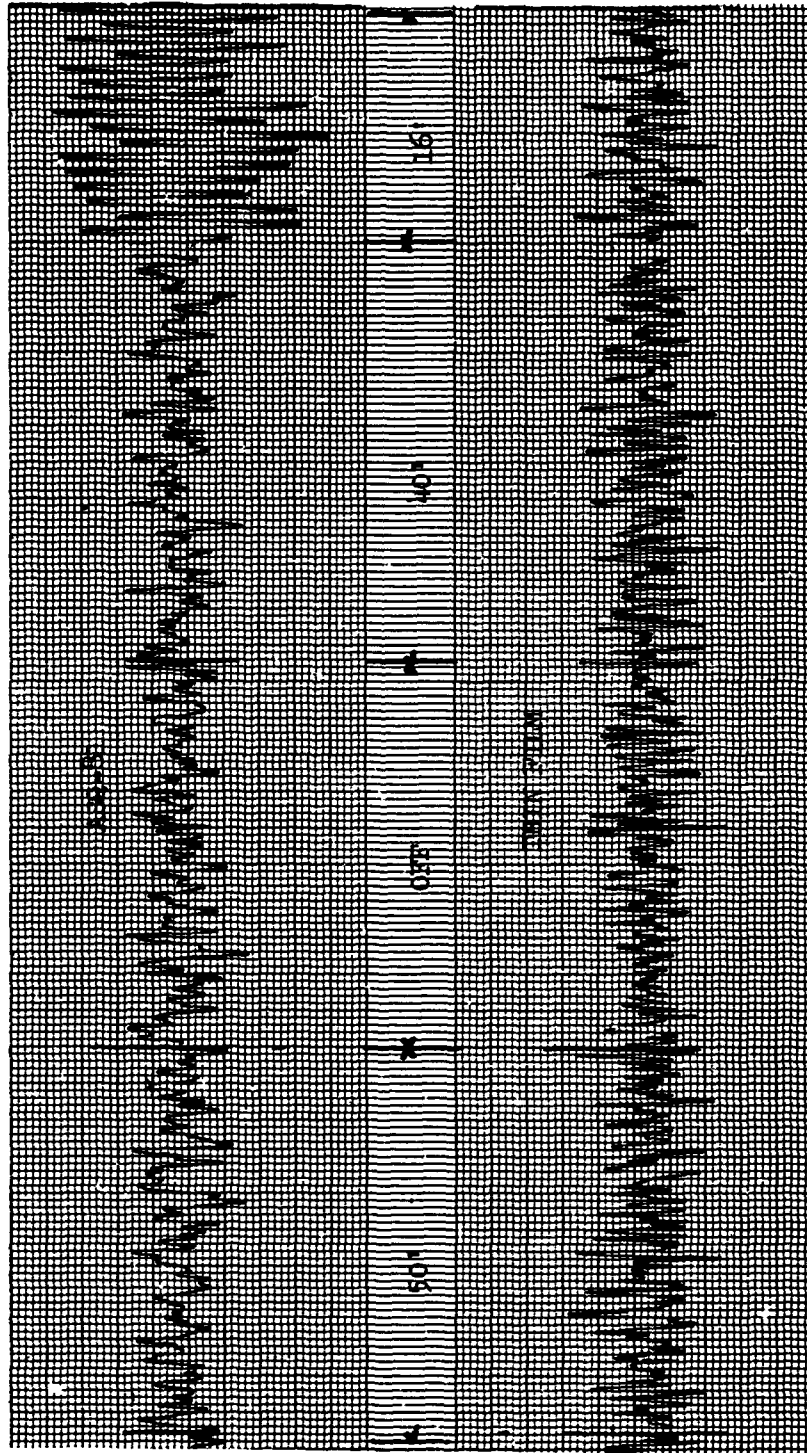
TIME (mm/sec.)

8 P.M. - 11 P.M.

FIGURE 16



RYE CANYON NEAR GROUND TEST DATA
GAMMA SLINGER @ 16 FT, 40 FT & 50 FT

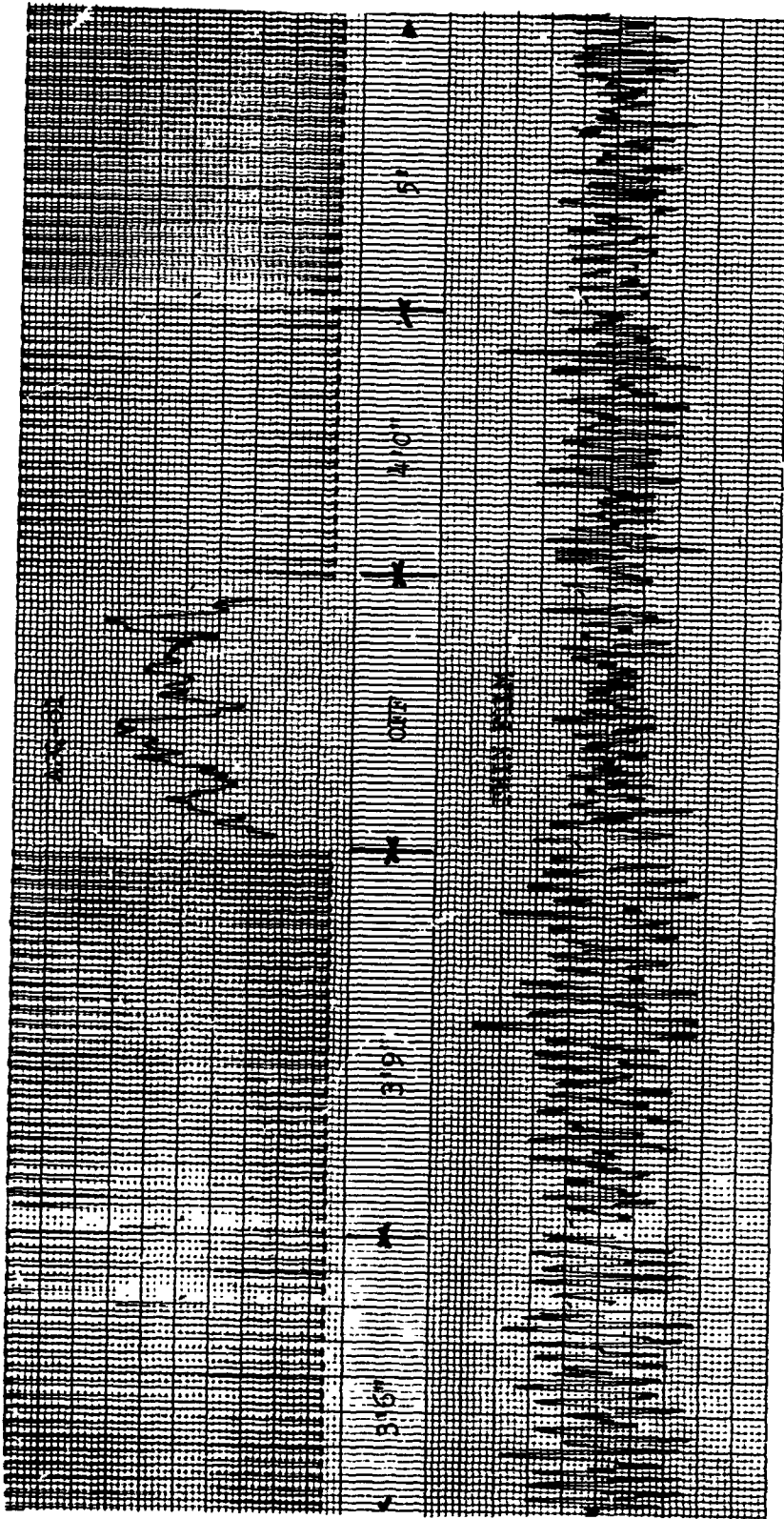


→ TIME (mm/sec.)

8 P.M. - 11 P.M.

FIGURE 17

RYE CANYON BALLOON TEST DATA
GAMMA SLINGER 5FT AND LESS

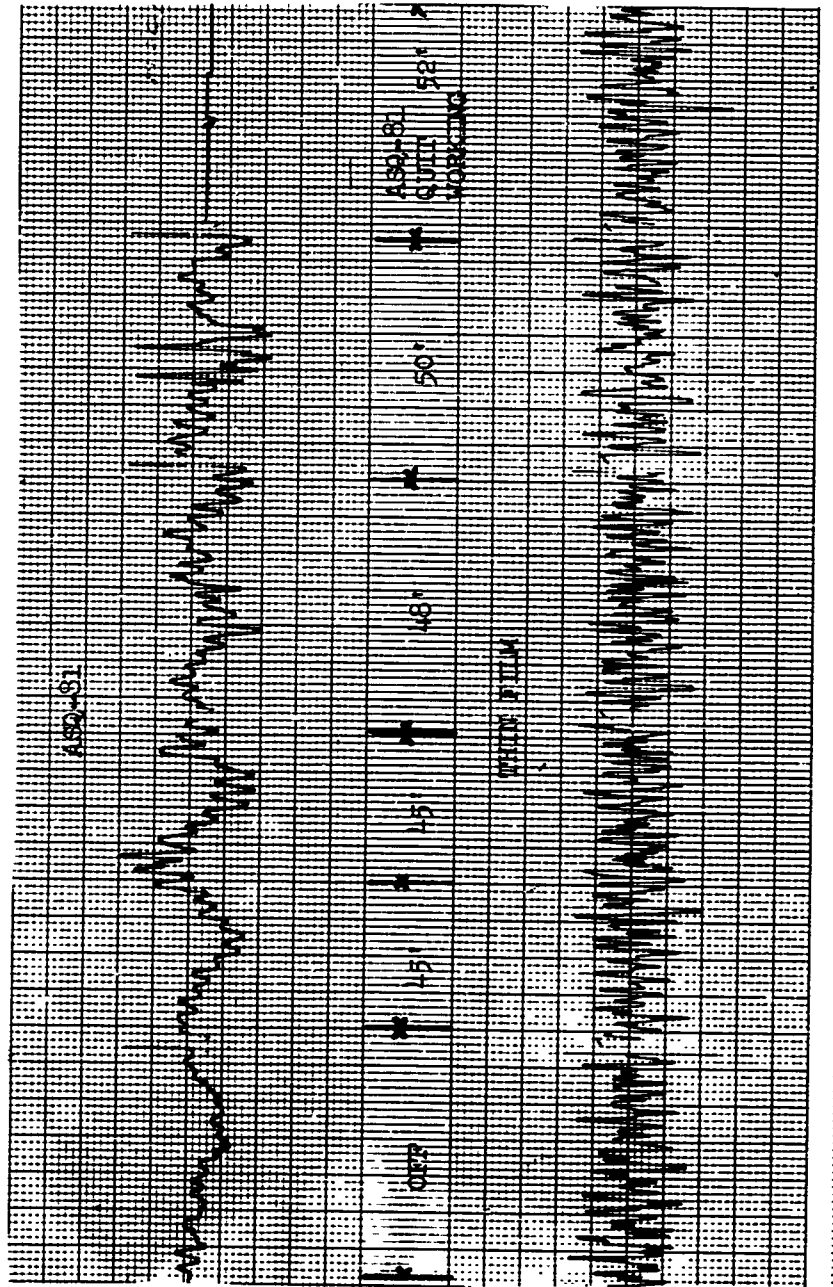


↑ TIME (min/sec.)

2 P.M. 1/4 P.M.

FIGURE 18

**RYE CANYON BALLOON TEST DATA
GAMMA SLINGER - 45 FT-50 FT**



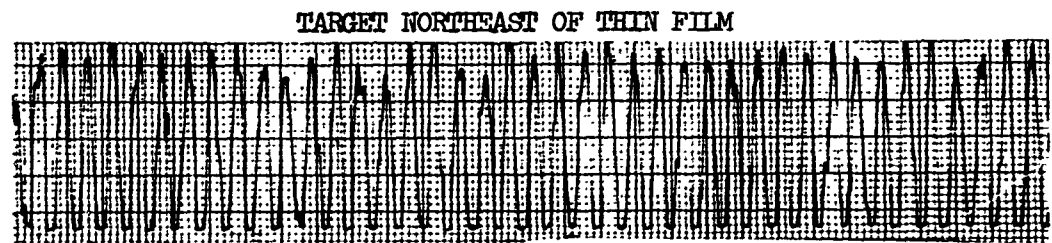
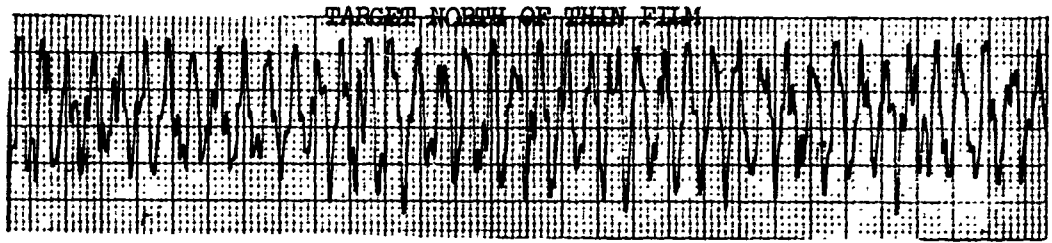
LR 24792

→ TIME (mm/sec.)

2P.M./4P.M.

FIGURE .19

THIN FILM/TARGET ORIENTATION DATA
N. NE, E & SE



→ TIME (mm/sec.)

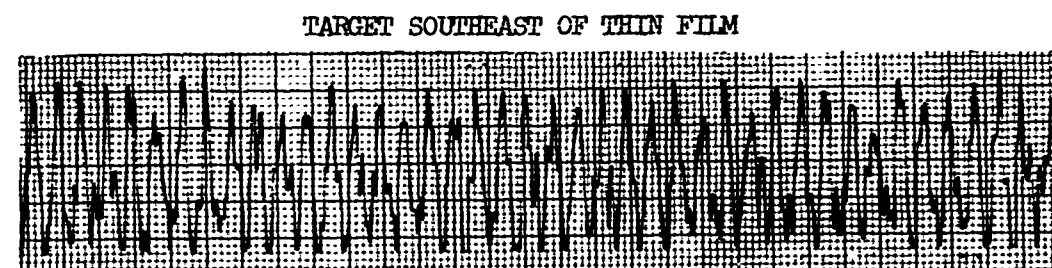
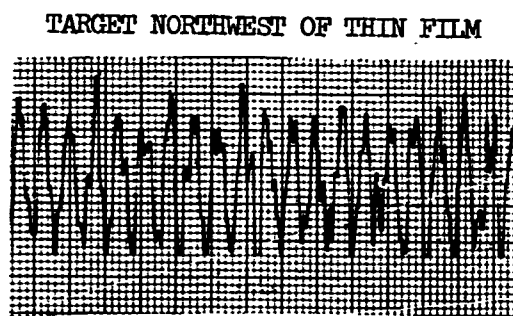
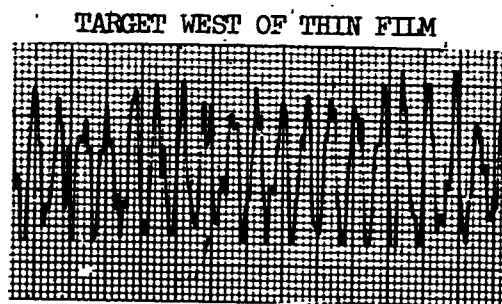
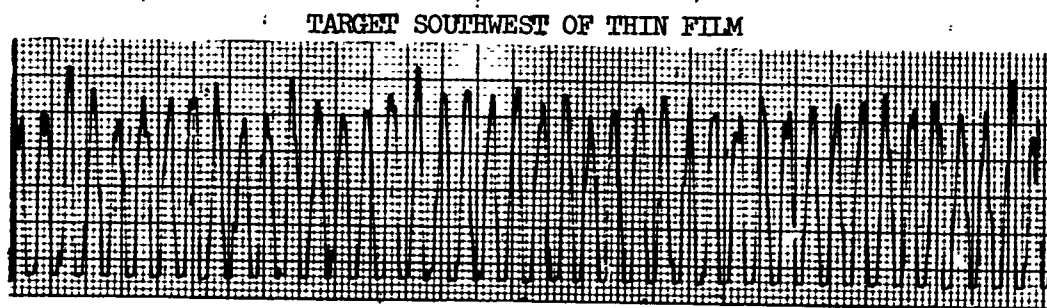
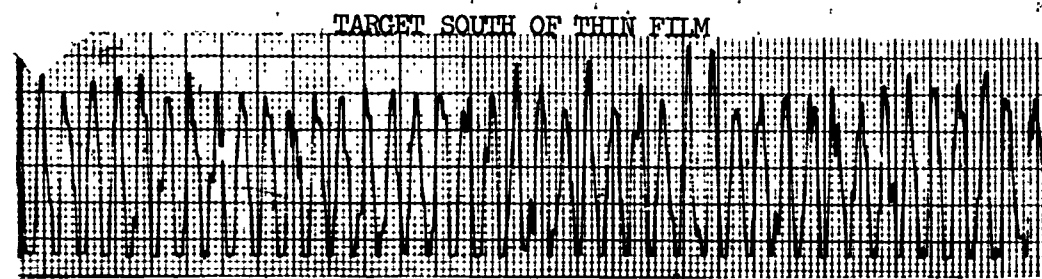


FIGURE 20

THIN FILM/TARGET ORIENTATION DATA
S, SW, W & NW



→ TIME (mm/sec.)

FIGURE 21

that, in the area in which the tests were conducted, northeast and 180° (or southwest) from that heading gives the most consistent, smoothest and greatest amplitude signal. However, if further tests of this nature were conducted in various geographical areas and more points of the compass used a different conclusion might be drawn. It should be noted though that most of the sensitivity tests conducted under this contract were made with a N-S target to sensor heading.

Substantial additional recorded sensitivity comparison data acquired under this contract have been retained in Lockheed files and is available for Office of Naval Research inspection and use.

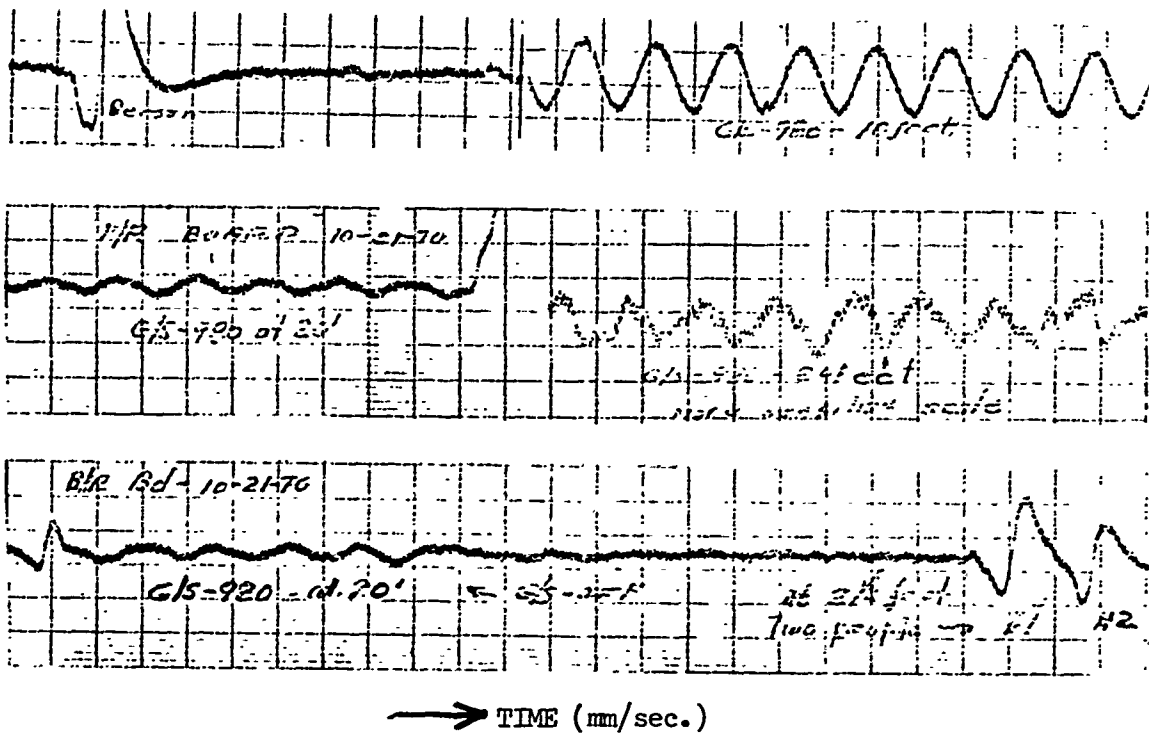


ROD SENSOR POTENTIAL

The following data and discussion considers the potential of the rod sensor on the basis of the demonstrated detection potential of the thin film approach when using a thin film square chip. Figure 22 shows the results of tests conducted in the fall of 1970 (with the same gamma slinger target used in this contract test program) indicating a high quality signal to noise ratio (about 4/1) at a distance of 20 feet.

The magnetic cube law extrapolates this performance to a unity (1/1) or MDS signal to noise ratio at a distance of 29 feet. This compares favorably with the ASQ-81 data of Figures 2 and 3. Achievement of similar performance with the presently used rod sensor (compatible with the 3-axis sum/square concept) requires incorporation of pump and bipolar detection improvements. As an example, improved performance can be attained by replacement of the present unshielded high impedance pump with a shielded low impedance pump such as previously used.

SELF-PUMPED SQUARE CHIP DATA SAMPLES
(NO MOTION COMPENSATION)



NOTE: This performance was secured with a high gain phase locked loop using the original square chip thin film rather than the rod type.

FIGURE 22

MOTION COMPENSATION 3-AXIS SUM/SQUARE DATAGeneral

The AN/ASA-65 three axis unit, each unit being exactly at 90° to each other, is utilized in the P-3C as a compensation device for the AN/ASQ-81 magnetometer system. It provides three independent orthogonal outputs which are individually applied to ASQ-81 compensation coils. In this research program, tests were conducted using this AN/ASA-65 for simplicity and demonstration of the proposed technique. The test point terminals for each of the three ASA-65 sensor legs were monitored and the resultant data plotted as a function of orientation angle in the earth's field. The sensor data was first obtained with one axis vertical and then skewed with no axis vertical. The curves drawn in Figures 23 and 24 are derived from the data given in Figures 25 and 26.

Vertical Axis Data

Figure 23 illustrates very little vertical axis response to rotation and typical sin/cos response of the other two sensors. The square root of the sum of the individual squares (F) shows a maximum variation of 0.15 volts for 360° rotation while the individual sensors show a variation of 6.5 volts. Over certain angle increments - such as from 300° to 360° and 360° to 60° , (F) shows no discernible variation. It is believed that the use of sensor derivative coupling in sensor outputs would further reduce amplifier dynamic range by virtue of limiting sensor output to dynamic field changes.

3-AXIS TEST DATA (ONE AXIS VERTICAL)

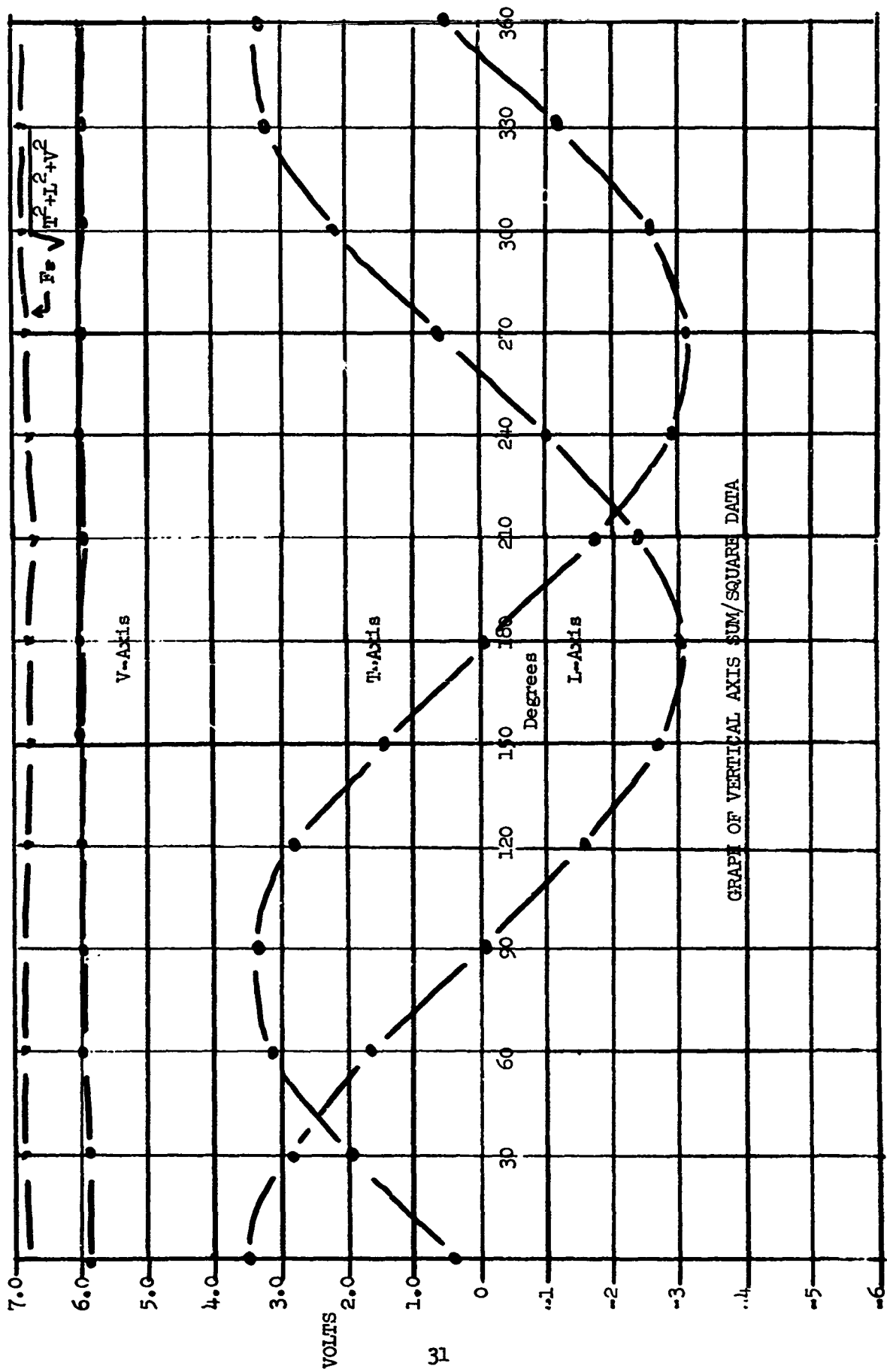


FIGURE 23

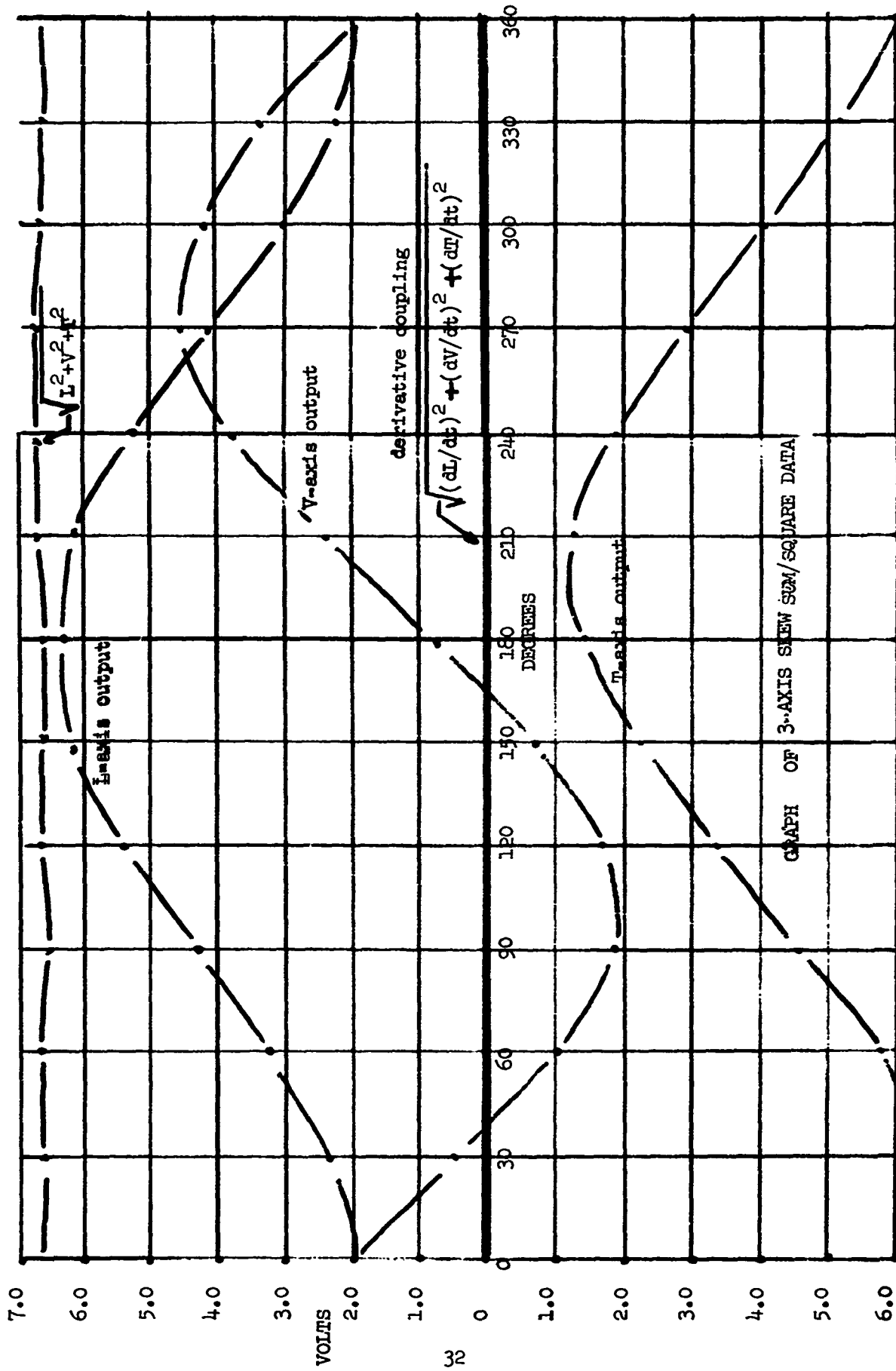


FIGURE 24

3-AXIS CONCEPT VALIDATION
DATA (V-AXIS: VERTICAL)

DEGREES	V-AXIS	T-AXIS	L-AXIS
000	5.9	4.0	3.50
030	5.95	1.96	2.86
060	5.9	3.05	1.60
090	5.9	3.35	-0.10
120	5.9	2.70	-1.65
150	5.95	1.40	-2.75
180	5.9	- .30	-3.05
210	5.9	-1.85	-2.42
240	5.9	-2.95	-1.15
270	5.9	-3.20	0.60
300	5.95	-2.66	2.15
330	5.9	-1.30	3.20
360	5.9	0.40	3.50
000	5.9	0.40	3.5
030	5.9	1.96	2.85
060	5.94	3.05	1.61
120	5.95	3.35	0.05
150	5.96	2.78	1.65
180	5.97	1.40	2.75
210	5.98	0.25	3.06
240	5.99	1.80	2.40
270	5.98	2.97	1.15
300	5.97	3.20	0.55
360	5.94	1.30	3.20
370	5.90	0.40	3.50

Figure 25

3-AXIS CONCEPT VALIDATION
DATA (V-AXIS-SKEWED)

DEGREES	VOLTS		
	T-AXIS	L-AXIS	V-AXIS
000	6.10	1.98	1.98
030	6.26	2.30	0.30
060	5.85	3.20	1.12
090	4.60	4.20	1.85
120	3.45	5.42	1.72
150	2.25	6.15	0.75
180	1.45	6.25	0.75
210	1.30	6.15	2.35
240	1.84	5.27	3.78
270	2.85	4.15	4.50
300	4.10	3.00	4.20
330	5.25	2.25	3.40
360	6.10	1.98	1.90
000	6.10	1.98	1.98
030	6.20	2.30	0.30
060	5.85	3.19	1.13
090	4.58	4.20	1.86
120	3.50	5.40	1.71
150	2.25	6.17	0.75
180	1.46	6.25	0.78
210	1.33	6.15	2.33
240	1.85	5.25	3.80
270	2.85	4.14	4.50
300	4.12	4.14	4.50
330	5.30	2.27	3.40
360	6.10	1.98	1.98

Figure 26

3-Axis Skew Data

Figure 24 illustrates sin/cos orientation response for all three sensors with amplitude variances up to 6.5 volts. The total field calculation of (F) shows again about 0.15 volt variation for 360° rotation. In this test, another set of data were taken using derivative/capacity coupling of the individual sensors. These data are given in Figure 27. In this derivative coupling test, the ASA-65 was rotated and the response recorded after a 1-second delay. During the first half second after an incremental change in angle, the individual sensors indicated a transient response as shown which quickly reduced to zero.

3-AXIS DERIVATIVE COUPLING DATA

DEGREES	VOLTS*		
	T	L	V
000	0-(0.00)	0-(0.00)	0-(0.00)
030	0-(.030)	0-(0.50)	0-(-1.86)
060	0-(.270)	0-(0.99)	0-(-1.50)
090	0-(1.20)	0-(1.42)	0-(0.87)
120	0-(1.50)	0-(1.42)	0-(0.20)
150	0-(1.40)	0-(0.98)	0-(1.20)
180	0-(0.86)	0-(0.35)	0-(1.70)
210	0-(0.30)	0-(-0.35)	0-(2.04)
240	0-(-0.55)	0-(-0.90)	0-(1.60)
270	0-(-1.15)	0-(-1.35)	0-(0.85)
300	0-(-1.40)	0-(-1.30)	0-(-0.15)
330	0-(-1.30)	0-(-0.96)	0-(-1.05)
360	0-(-0.90)	0-(-0.30)	0-(-1.60)

*PARENTHESES DATA INDICATES "EYEBALL" ESTIMATE OF TRANSIENT RESPONSE TO ANGLE INCREMENTS OF 30 DEGREES

Figure 27



Squaring Circuit Development

As described in Reference (1) Lockheed has developed under in-house Independent Research funding a low power electronic squaring circuit. Figure 28 is a data plot of the squaring circuit output versus input. A sine wave generator was used in conjunction with a phase splitter to supply equal amplitude but phase reversed inputs to both sides of the squaring circuit. The load resistor output was a second harmonic sine wave whose base level was nominally equal to one-half the supply voltage. Thus, as the input varied, the D.C. mid-level of this second harmonic varied and a capacitor between the output and ground provided a filtered D.C. level which was monitored by a Simpson 303 meter to observe the data plotted in the figure. The phase inverter leads were reversed as shown by the plot to check the squaring function for phase reversal characteristics.

The test results shown in Figure 28 support the conclusion that not only is the sum/square concept solid but also that the sum/square concept appears feasible from an initial research standpoint. There are, however, limitations which relate to the degree to which three squaring channels can be matched, as well as the degree of 3-axis symmetry electronic and physical symmetry which can be achieved. It should be noted that the variability between solid state transistor and FET devices may pose a requirement for critical selective matching of components. For example, the initial squaring circuit developed by Lockheed involved a high component rejection rate. The problem of achieving 3-axis matching may impose a 95% rejection rate unless uniform component production can be achieved by tighter specifications. The Lockheed squaring circuit requires relatively little power compared to typical and commercially available squaring circuit modules.

TYPICAL SQUARING CIRCUIT DATA

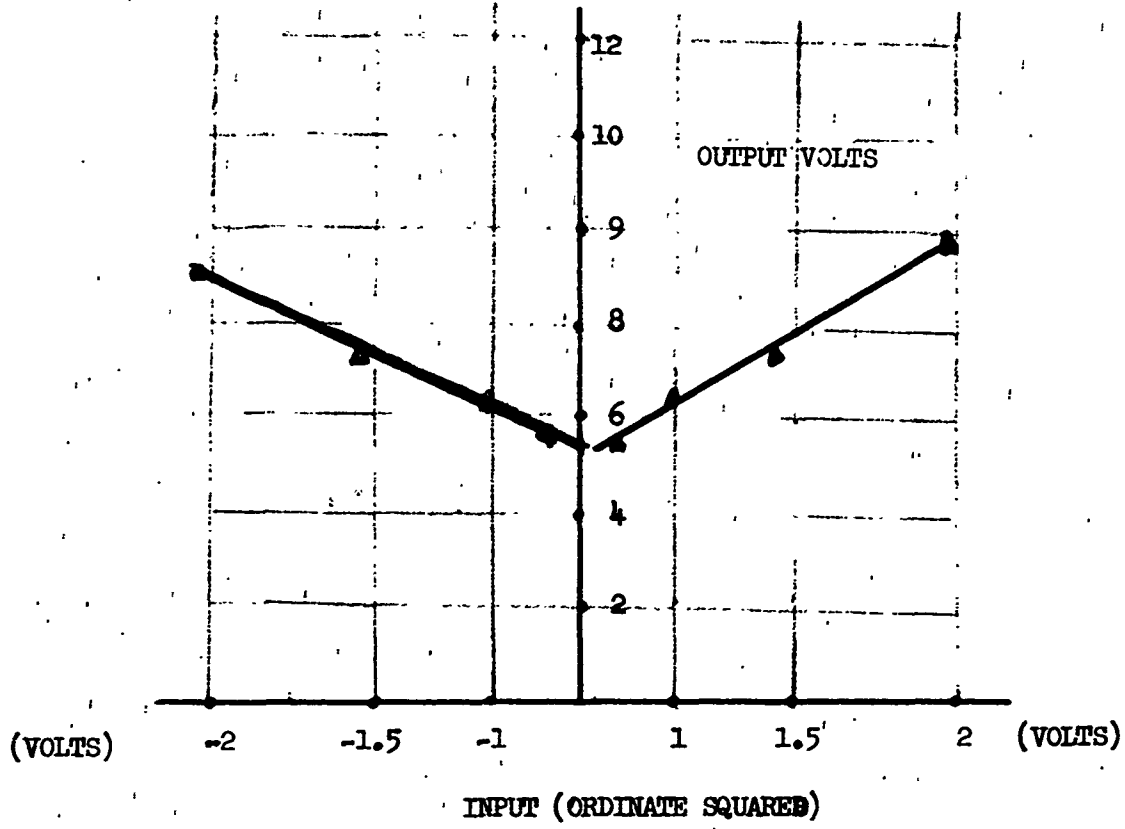


FIGURE 28

DISCUSSIONS: RESULTS, PROBLEM AREAS AND SOLUTIONSGeneral

The results of this program indicate that the sum/square function appears to lend itself to module development with status of the art components. This module could be designed to mate with either the ASA-65 or a 3-axis mini-rod configuration. Rod sensor sensitivity can probably be increased significantly by reduction of pump induced noise.

Sum/Square Research

Further effort in this area could be based upon use of available squaring modules which generally require higher power than the circuit developed by Lockheed. The Lockheed circuit however has been based upon FET items which have a wide variance in their electronic characteristics. It is an open question at this time whether three matched squaring channels can be better fabricated after conducting squaring circuit research or with use of commercially available squaring circuits. While this question is not completely resolved at this time, Lockheed independent research indicates that the 3-axis sum/square module can be assembled within status of the art components provided selective utilization of components is exercised. Such a sum/square module could be interfaced with the AN/ASA-65 as an expedient approach.

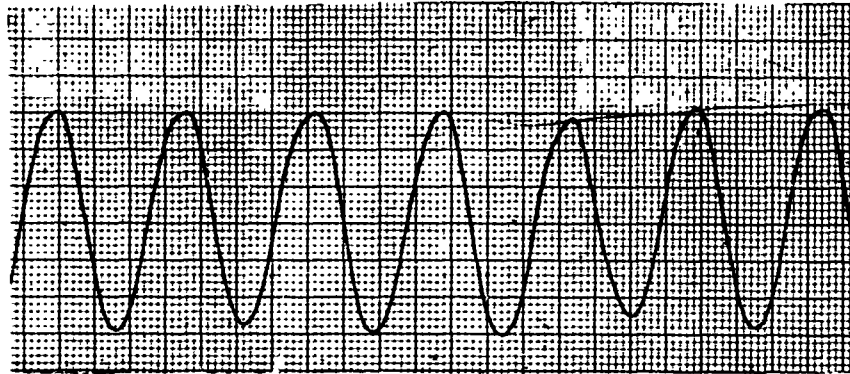
Sensor Potential

As indicated in the previous Figure 22 and the following Figure 29, square chip performance exceeds by a wide margin the performance

SELF PUMPED THIN FILM DATA

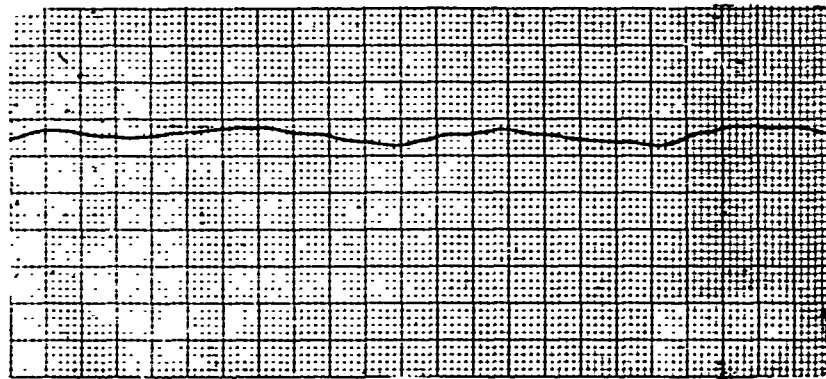
(This data secured with high gain phase locked loop.)

GAMMA
SLINGER ON
AT 10'

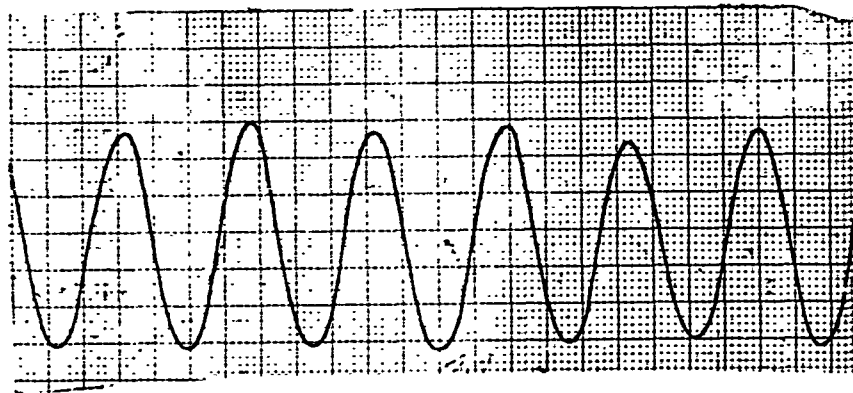


→ TIME (mm/sec.)

GAMMA
SLINGER
OFF



GAMMA
SLINGER
ON AT
10'



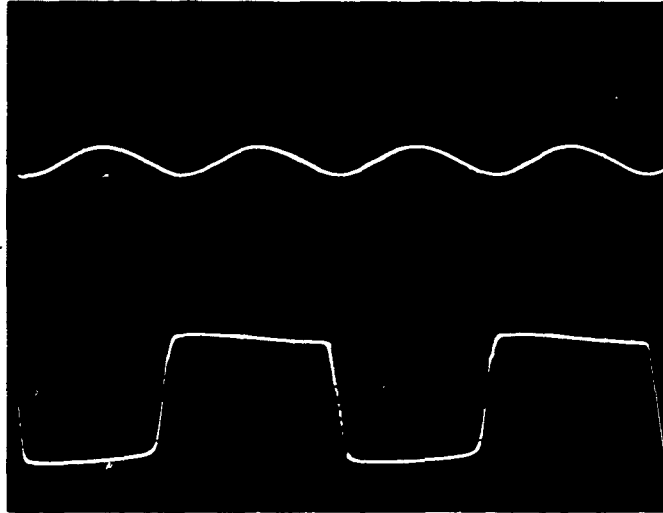
AUGUST 27, 1970

FIGURE 29

PUMP/SENSOR FEEDBACK

PUMP
OSCILLATOR
WAVEFORM
BEFORE SHORTING
OF SENSOR COIL

CORRELATOR
OUTPUT



PUMP
OSCILLATOR
WAVEFORM
WITH SENSOR
COIL SHORTED

CORRELATOR
OUTPUT

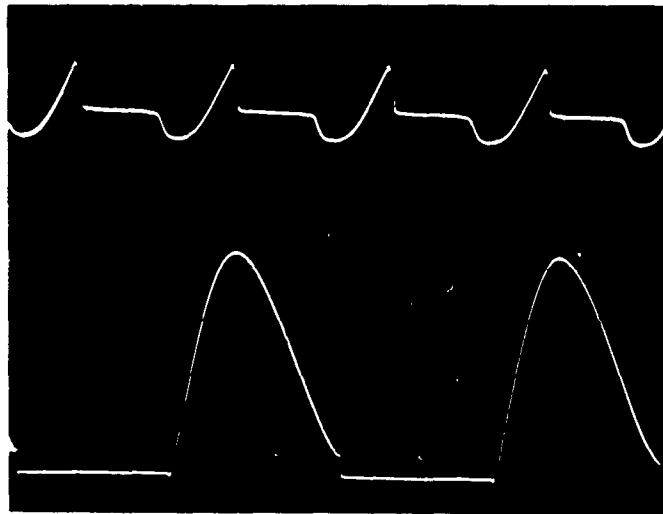


FIGURE 30

obtained by the rod sensor at this early stage of its development. (The data shown in Figure 29 was secured with the same gamma slinger target used in the other parts of this test program.) While these data were secured with a self-pumped square chip sensor, similar performance can be obtained with external pumping providing the pump phase reference is free of noise.

Noise Sources

In this first stage of rod sensor development, a high sensor drive level was used in order to increase the sensor response to a signal input. The sensor output was a high level unipolar pulse whose output at a relatively low impedance level exceeded the high impedance pump crystal oscillator output by about 30 db. In this first rod configuration, the unshielded high impedance low level output of the crystal oscillator was vulnerable to phase, amplitude, and frequency shifts due to temperature and sensor output feedback into the crystal oscillator. When either the sensor output or the oscillator output was shorted a substantial decrease in output noise level was observed. These observations indicate that the sensor and pump were not mutually independent. To test this further, the sensor coil was shorted out and a change was noted in the characteristics of the pump oscillator as indicated in Figure 30.

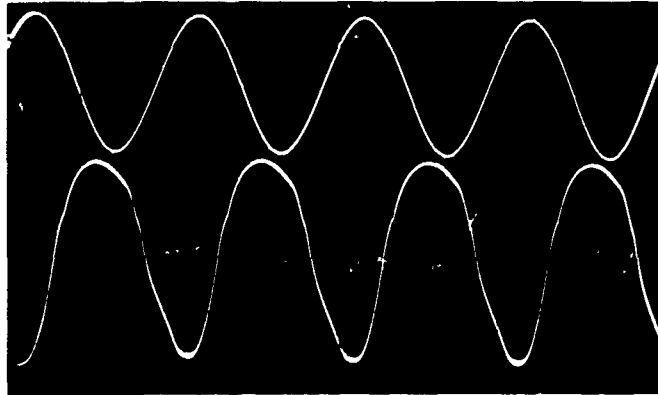
Rod Sensor Improvements

In earlier thin film externally pumped square chip compass work and in self-pumped square chip work, the pump action was at a relatively low impedance and therefore relatively independent

BIPOLAR OUTPUT CHARACTERISTICS

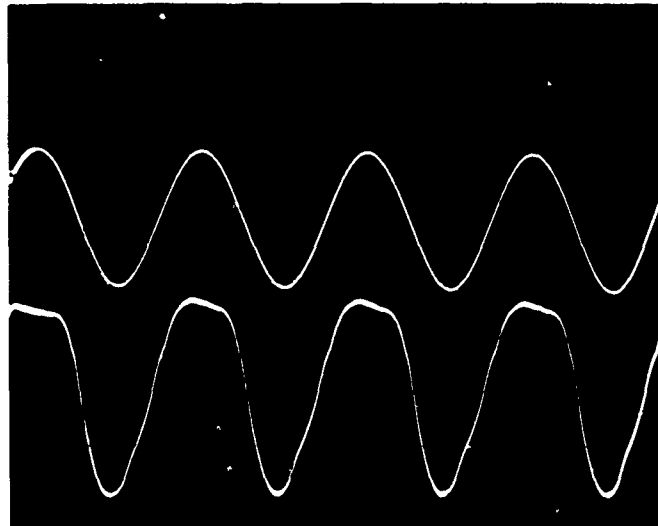
REFERENCE

OUT OF PHASE
SENSOR OUTPUT



REFERENCE

IN PHASE
SENSOR OUTPUT



REFERENCE

TYPICAL
SENSOR NULL
CHARACTER

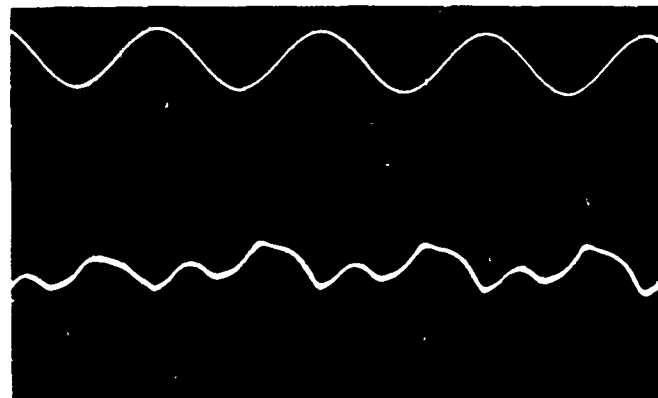


FIGURE 31

of noise shifts due to sensor feedback temperature, capacity pickup, and other forms of environmental noise. In these more sensitive systems, the sensor output was a low level bipolar output as contrasted to the high level unipolar characteristic of the rod used in this program. Lockheed has in its own research, however, determined a rod circuit whose output characteristics (shown in Figure 31) provide the bipolar characteristic which has been symptomatic of high sensor performance. In this Figure 31, the lower photo represents a sensor null corresponding to a certain orientation angle. The two upper photos represent in phase and out of phase sensor outputs caused by displacing the sensor to either side of the null angle. It is believed this bipolar rod coupled with shielded low impedance pump excitation could provide both compass and 3-axis sum/square capability.

Sensor Performance Shifts

In previous self-pumped and externally pumped chip designs, the sensor was phase locked so as to provide displacement compensation. Thus, if such a sensor were rotated about its axis, a response would take place during the rotation; after the rotation, the sensor would automatically bias itself to the most sensitive portion of its detection characteristic. In this program, based upon the 3-axis sum/square concept, this feature was not used. Therefore, in these tests, a critical interface existed between sensor orientation angle and any phase shifts in the operating point of the high impedance pump oscillator. While this pump was crystal controlled, finger touch of the crystal case caused very large noise fluctuations in sensor output. Further, the specification for such high



impedance crystals indicate the need for critical temperature stabilization. These considerations give reasons for some of the fluctuations in the rod sensor performance during this program. At this stage of research, the suitability and practicality of phase locking each sensor in a 3-axis sensor configuration poses certain factors; for example, the effect of such a design on the phased sum/square operation is not known, could lead to alignment complexity, and possibly increase system complexity. Further, it may be possible that the 3-axis sum/square technique does not require such phase locking to ensure maximum performance and it is possible that phase locking would degrade performance.

Core Materials

Lockheed studies indicate that considerations should be given to other materials and designs which may be superior to thin film devices. For example, tests indicate that the Q of thin film sensors normally used in compass and sensor research nominally falls between 6 and 10. Reference (2) and other source material indicate the possibility of securing a sensor Q as high as 140.

Total Field Sensor

The 3-axis total field concepts poses a dynamic range problem associated with the squaring function requirement. This problem requires a solution in order to achieve suitable sensitivity. Lockheed initial analysis of this problem indicates that a practical solution is available which provides sensitive linear detection in a manner that is compatible with the 3-axis sum/square motion compensation concept.



CONCLUSIONS

The results of this ONR sponsored program leads to the conclusion that a 3-axis motion compensated low power mini-magnetic sensor (Mini-Mad) appears feasible. Specific aspects of this conclusion are as follows:

- (1) A 3-axis Mini-Mad sum/square sensor system can be assembled with available state of the art components and materials.
- (2) The ultimate sensitivity capabilities of the Mini-Mad configuration cannot at this time be predicted accurately. However, a 0.1 to 0.5 gamma sensitivity level does appear achievable in a system.
- (3) The sensitivity comparison tests of the rod thin film versus the AN/ASQ-81 showed the ASQ-81 to be far superior in all noise environments in which the tests were conducted. Range comparisons of 1/4, 1/2.7, 1/4, 1/7.5 in the various type tests conducted indicates that a nominal 1 to 4 ratio was demonstrated for the rod sensor.
- (4) The sensitivity tests conducted on the square chip thin film showed a gamma slinger pickup at 29 feet range versus a maximum of 45 feet for the ASQ-81 tested at a different time and environment. This gives a range ratio of 1 to 1.55. There is no reason to believe that this same capability cannot be achieved in the rod sensor.

RECOMMENDATIONS

Further advancement of a motion compensated Mini-Mad sensor system should include further 3-axis sensor research along with sensor element considerations. In addition, the scope of the research program should include the total field sensor concept. The following specific areas are recommended for further effort:

- (1) Conduct literature search, historical and contemporary work that may constructively apply to motion compensated Mini-Mad feasibility.
- (2) Derive and test a "quick reaction" total concept model by fabrication of a sum/square module which mates with the 3-axis ASA-65 rod system.
- (3) Investigate by analysis, research and tests the sensor detection potential and refine mini-rod sensor, other sensor elements and related circuits for improved sensitivity and noise reduction.
- (4) Conduct analysis of design requirements to meet dynamic range requirements for 3-axis sum/square function.
- (5) Conduct research and analysis on the total field sensor approach.
- (6) Generate a total program plan for Mini-Mad systems that puts into perspective the technical, research, development, and operational requirements for advancement of Mini-Mad systems. This plan should include the following tasks:

MOTION COMPENSATED MINI-MAD
PROGRAM TASKS

Research

Operational Analysis
Sensitivity Analysis

Application Study
Communication Interfaces
Environmental Limitations
(Temperatures, Shock,
etc.)

MAD Signal Study
Aircraft Noise
Solar/Global Noise

Applied Research

Sensor Circuits
3-Axis Sensor
Construction
Signal Processing
Sensor Drive Techniques
Core Winding Techniques
Core Materials

Total Field Sensor

Development

Sum/Square Module
Amplifier/Filter
Systems
Correlator Circuits
Pump Drive Circuits
Filter Circuits

BIBLIOGRAPHY REFERENCES

1. Mini-Magnetometer Motion Compensation, Lockheed Report No. 24530,
14 May 1971.
2. Principles of Radio Engineering by Glasgow, McGraw Hill, 1936



APPENDIX A
FACILITY/TEST PHOTOGRAPHS

This appendix consists of photographs of the Lockheed Rye Canyon Research Center Magnetics and Burbank test facilities used in this program other than illustrated in Figure 1.

Figure A-1: a pressured balloon non-magnetic material facility at Rye Canyon. This facility houses the equipment and fixtures used in AN/ASQ-81 and other MAD and compensation system testing programs. Remote control of equipment is exercised in the companion facility shown in Figure A-2.

Figure A-2: Rye Canyon test and control building. This facility not only houses the control equipment for the balloon facility, but also houses other recording and test equipment for MAD R & D.

Figure A-3: This interior view of the balloon test facility shows the AN/ASQ-81 installed in the maneuver cradle fixture with the Mini-Mad sensor near the ASQ-81 sensor head.

Figure A-4: This photo illustrates the Burbank submarine model target track facility and gamma slinger located in the foreground with the ASQ-81 and thin film sensor in the background.

Figure A-5: This closeup photo of the target track shows a pipe target on the movable dolly and the drive motor in the foreground.



FIGURE A-1 EXTERIOR - RYE CANYON BALLOON MAGNETICS TEST FACILITY

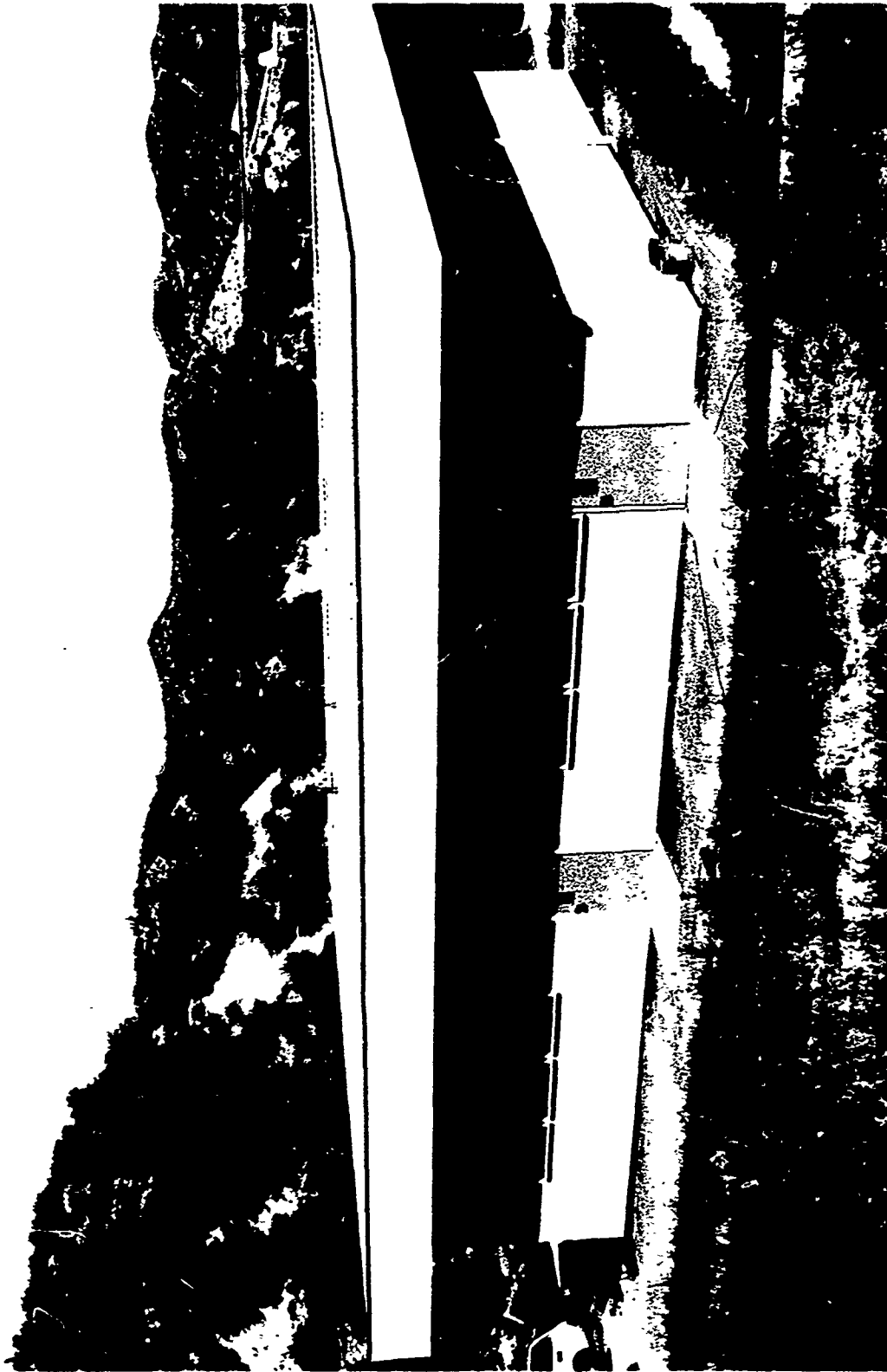


FIGURE A-2. MAGNETICS TEST AND CONTROL BUILDING (RYE CANYON TEST FACILITY)

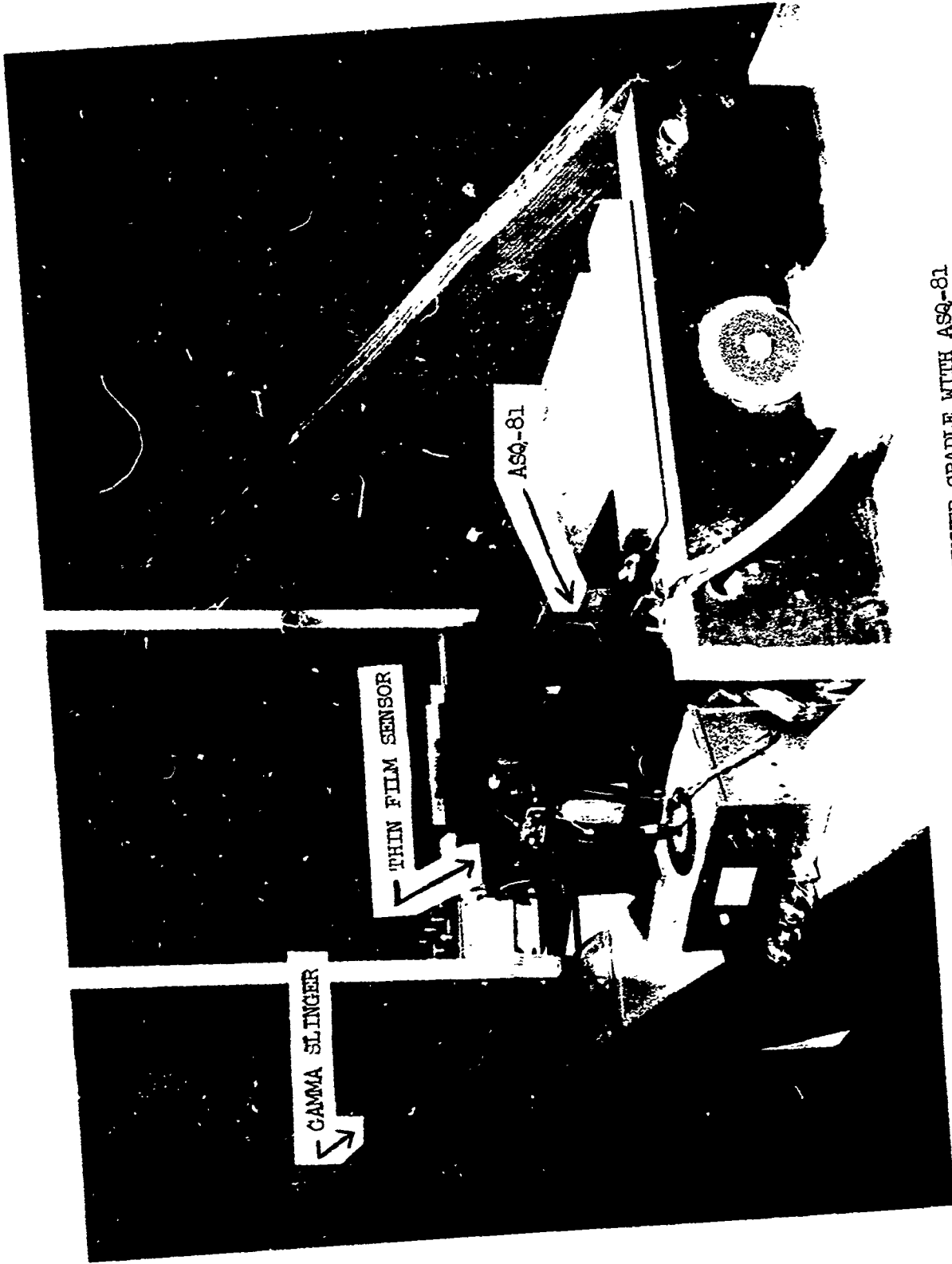


FIGURE A-3 BALLOON INTERIOR MANEUVER CRADLE WITH ASQ-81
& THIN FILM SENSOR



FIGURE A-4 MODEL TARGET TRACK (BURBANK TEST FACILITY)